

Generalized Onsager reciprocal relations of charge and spin transport

Guan-Hua Huang,^{1,2,*} Hui Tang,^{3,*} Shizhong Zhang,⁴ Zhongbo Yan,^{5,†} and Zhigang Wu^{2,‡}

¹Hefei National Laboratory, Hefei 230088, China

²Quantum Science Center of Guangdong-Hong Kong-Macao Greater Bay Area (Guangdong), Shenzhen 508045, China

³Shenzhen Institute for Quantum Science and Engineering,

Southern University of Science and Technology, Shenzhen 518055, China

⁴Department of Physics and HKU-UCAS Joint Institute for Theoretical and Computational Physics at Hong Kong, University of Hong Kong, Hong Kong, China

⁵Guangdong Provincial Key Laboratory of Magnetoelectric Physics and Devices, School of Physics, Sun Yat-Sen University, Guangzhou 510275, China

(Dated: June 19, 2025)

In spin-orbit-coupled systems the charge and spin transport are generally coupled to each other, namely a charge current will induce a spin current and vice versa. In the presence of time-reversal symmetry \mathcal{T} , the cross-coupling transport coefficients describing how one process affects the other are constrained by the famous Onsager reciprocal relations. In this paper, we generalize the Onsager reciprocal relations of charge and spin transport to systems that break the time-reversal symmetry but preserve a combined symmetry of \mathcal{T} and some other symmetry operation \mathcal{O} . We show that the symmetry or antisymmetry of the cross-coupling transport coefficients remains in place provided that the operator \mathcal{O} meets certain conditions. Among many candidate systems where our generalized Onsager relations apply, we focus on a conceptually simple and experimentally realized model in cold atomic systems for explicit demonstration and use these relations to predict highly non-trivial transport phenomena that can be readily verified experimentally.

The Onsager reciprocal relations [1, 2], which reveal a fundamental symmetry or antisymmetry between the cross-coupling transport coefficients in time-reversal symmetric systems, are among the most important physical laws governing irreversible processes. When a system is perturbed slightly from equilibrium by a set of forces F_j that are conjugate to generalized coordinates x_j , the induced current $J_i \equiv dx_i/dt$ corresponding to x_i can be expressed as $J_i = \sum_j L_{ij} F_j$ via the linear response theory. The Onsager reciprocal relations then dictate that $L_{ij} = \pm L_{ji}$ in the presence of time-reversal symmetry, where the $+$ ($-$) sign corresponds to the product $x_i x_j$ being time-reversal even (odd) [3]. Connecting microscopic reversibility to thermodynamically irreversible processes, Onsager relations have provided deep insights into a wide range of transport phenomena [4–15], including thermoelectric phenomena, superfluidity, and spintronics.

Indeed, the establishment of Onsager reciprocal relations has played a pivotal role in addressing one of the long-debated problems in spintronics, namely the proper definition of the spin current [16–21]. Conventionally, the single-particle spin current operator is defined as $\hat{j}_{\text{conv}}^s = \frac{1}{2}\{\hat{s}_z, \hat{j}^c\}$ [22, 23], where $\hat{s}_z = \frac{1}{2}\sigma_z$ is the spin operator and $\hat{j}^c = d\hat{r}/dt$ is the single-particle charge (or mass) current operator. A central deficiency of this definition is that it does not correspond to any generalized coordinate and thus no conjugate force exists to generate this spin current, which in turn makes it impossible to establish the Onsager reciprocal relations in coupled charge and spin transport. To remedy this, Shi *et al.* [16] observed that the appropriate generalized coordinate for the spin transport is the spin displacement operator $\hat{r}\hat{s}_z$ and so the spin current can be defined as the corresponding total flux $\hat{j}^s = d(\hat{r}\hat{s}_z)/dt$, in much the same way that

the charge current is defined as the total flux of the charge displacement \hat{r} . Thus, in response to the external potential $\delta V = -\mathbf{F}^c \cdot \hat{r} - \mathbf{F}^s \cdot (\hat{r}\hat{s}_z)$, the charge current \mathbf{J}^c and the spin current \mathbf{J}^s are determined by linear response theory as

$$J_\mu^c = \sum_\nu (\sigma_{\mu\nu}^{cs} F_\nu^s + \sigma_{\mu\nu}^{cc} F_\nu^c); \quad (1)$$

$$J_\mu^s = \sum_\nu (\sigma_{\mu\nu}^{ss} F_\nu^s + \sigma_{\mu\nu}^{sc} F_\nu^c), \quad (2)$$

where \mathbf{F}^c and \mathbf{F}^s are forces conjugate to \hat{r} and $\hat{r}\hat{s}_z$ respectively, and $\{\sigma_{\mu\nu}^{ss}, \sigma_{\mu\nu}^{cc}, \sigma_{\mu\nu}^{sc}, \sigma_{\mu\nu}^{cs}\}$ are a set of dc transport tensor coefficients [24]. Assuming time-reversal symmetry, the Onsager reciprocal relations between the charge-spin cross-coupling transport coefficients are then

$$\sigma_{\mu\nu}^{sc} = -\sigma_{\nu\mu}^{cs}, \quad (3)$$

where the antisymmetry comes from the fact that the product $\hat{r}_\mu(\hat{r}_\nu\hat{s}_z)$ is time-reversal odd. This alternative definition of spin current and the associated Onsager relations have been influential for several reasons [25–28]. For example, the spin Hall conductivity σ_{xy}^{sc} , traditionally challenging to measure, can now be deduced from the electric current induced by a spin force in light of the Onsager relations in Eq. (3).

The Onsager reciprocal relations are fundamentally predicated on the time-reversal symmetry, yet this symmetry is broken by magnetism in many systems actively studied for spintronics [29–33]. Therefore, to what extent these relations can still be established in such systems remains a pressing open question [34–36]. The critical importance of resolving this question is exemplified by recent contradictory findings in antiferromagnet YbMnBi₂, where independent studies have reported both the preservation and the violation of the Onsager reciprocal relations regarding the anomalous electric and thermoelectric conductivity tensors [14, 37].

In this Letter, we generalize the Onsager reciprocal relations of spin and charge transport to systems that break the time-reversal symmetry but preserve a combined symmetry of \mathcal{T} and some other symmetry operation \mathcal{O} . We first show that relations similar to Eq. (3) still hold provided that \hat{r}_μ and \hat{s}_z are invariant or change sign under the operation \mathcal{O} , i.e.,

$$\mathcal{O}^{-1}\hat{r}_\mu\mathcal{O} = (-1)^{I_\mu}\hat{r}_\mu; \quad \mathcal{O}^{-1}\hat{s}_z\mathcal{O} = (-1)^{I_s}\hat{s}_z, \quad (4)$$

where the indices I_μ and I_s take the value of 0 or 1.

We begin with the Kubo formulas of the charge-spin cross-coupling transport coefficients at finite frequency

$$\sigma_{\mu\nu}^{\text{sc}}(\omega) = i \int_0^\infty dt \langle [\hat{J}_\mu^s(t), \hat{R}_\nu^c(0)] \rangle e^{i\omega t}, \quad (5)$$

$$\sigma_{\nu\mu}^{\text{cs}}(\omega) = i \int_0^\infty dt \langle [\hat{J}_\nu^c(t), \hat{R}_\mu^s(0)] \rangle e^{i\omega t}, \quad (6)$$

where $\langle \dots \rangle$ stands for a statistical average at finite temperatures and an expectation value with respect to the ground state $|\Phi\rangle$ at zero temperature. Here $\hat{R}_\nu^c = \sum_j \hat{r}_{j,\nu}$ and $\hat{R}_\mu^s = \sum_j \hat{r}_{j,\mu} \hat{s}_{j,z}$ are the many-body charge and spin displacement operators respectively, and $\hat{J}_\nu^c = d\hat{R}_\nu^c/dt$ and $\hat{J}_\mu^s = d\hat{R}_\mu^s/dt$ are the corresponding charge and spin current operators. As usual, the Heisenberg operators such as $\hat{J}_\mu^s(t)$ is given by $\hat{J}_\mu^s(t) = e^{i\hat{H}t} \hat{J}_\mu^s(0) e^{-i\hat{H}t}$, where \hat{H} is the Hamiltonian of the system.

For brevity, we derive the generalized Onsager relations for the system in the ground state only as the finite temperature extension is straightforward. Assuming the \mathcal{OT} invariance of the ground state, i.e., $\mathcal{OT}|\Phi\rangle = e^{i\theta}|\Phi\rangle$, and keeping in mind that \mathcal{OT} is an antiunitary operator, we have $\langle \Phi | \hat{A}^\dagger | \Phi \rangle = \langle \Phi | \mathcal{OT} \hat{A} (\mathcal{OT})^{-1} | \Phi \rangle$ for any operator \hat{A} . Now we take $\hat{A} = \hat{R}_\nu^c(0) \hat{R}_\mu^s(t)$ and first observe that

$$\mathcal{OT} \hat{R}_\nu^c(0) (\mathcal{OT})^{-1} = (-1)^{I_\nu} \hat{R}_\nu^c(0) \quad (7)$$

due to the \mathcal{O} operation in Eq. (4) and the time-reversal invariance of $\hat{R}_\nu^c(0)$. Furthermore, since the antiunitary \mathcal{OT} operator commutes with \hat{H} we find

$$\begin{aligned} \mathcal{OT} \hat{R}_\mu^s(t) (\mathcal{OT})^{-1} &= e^{-i\hat{H}t} \mathcal{OT} \hat{R}_\mu^s(0) (\mathcal{OT})^{-1} e^{i\hat{H}t} \\ &= (-1)^{I_\mu + I_s + 1} \hat{R}_\mu^s(-t), \end{aligned} \quad (8)$$

where we again used Eq. (4) in the second line. Putting these together, we find

$$\langle \Phi | \hat{R}_\mu^s(t) \hat{R}_\nu^c(0) | \Phi \rangle = (-1)^{I_{\mu\nu}} \langle \Phi | \hat{R}_\nu^c(t) \hat{R}_\mu^s(0) | \Phi \rangle, \quad (9)$$

where the time-translation symmetry is used for the expectation value and $I_{\mu\nu} \equiv I_\mu + I_\nu + I_s + 1$. Taking the derivative on both sides further yields

$$\langle \Phi | \hat{J}_\mu^s(t) \hat{R}_\nu^c(0) | \Phi \rangle = (-1)^{I_{\mu\nu}} \langle \Phi | \hat{J}_\nu^c(t) \hat{R}_\mu^s(0) | \Phi \rangle. \quad (10)$$

Lastly, substituting Eq. (10) into Eqs. (5)-(6) we arrive at the generalized Onsager reciprocal relations of charge and spin transport

$$\sigma_{\mu\nu}^{\text{sc}}(\omega) = (-1)^{I_{\mu\nu}} \sigma_{\nu\mu}^{\text{cs}}(\omega). \quad (11)$$

Several comments are now in order. First, we recover the usual Onsager relations in Eq. (3) in the presence of time-reversal symmetry by setting \mathcal{O} as an identity operator and taking the zero-frequency limit. Second, the conditions for operation \mathcal{O} in Eq. (4) can actually be somewhat relaxed. It is clear that the transformation of the commutators in Eqs. (5)-(6) under \mathcal{O} remains the same even if the right-hand sides of the equations in Eq. (4) include an additional finite constant. This means that any \mathcal{O} operation leaving \hat{r}_μ and \hat{s}_z invariant or with a changed sign *up to a constant* still leads to the generalized Onsager relations in Eq. (11). Third, suitable \mathcal{O} operations fall into three categories: (i) pure spatial operations such as spatial inversion \mathcal{P} , π -rotation about any Cartesian axis and lattice translation (ii) pure spin operations such as any spin rotation around z -axis and π -rotation around x or y -axis; and (iii) space-spin operations including any combination of those in (i) and (ii), as well as mirror and glide symmetries. Lastly, in cases where the system has multiple \mathcal{OT} symmetries, we must examine the generalized Onsager relations corresponding to each and every \mathcal{O} operation. If two \mathcal{O} operations lead to contradictory relations with respect to $\sigma_{\mu\nu}^{\text{sc}}(\omega)$ and $\sigma_{\nu\mu}^{\text{cs}}(\omega)$, we can immediately draw the conclusion from Eq. (11) that both must vanish identically.

The generalized Onsager reciprocal relations derived above are expected to find broad application, particularly in antiferromagnets where zero net magnetization is enforced by specific forms of \mathcal{OT} symmetry [38, 39]. Notably, many experimentally realized antiferromagnets (see, e.g., Table I in Ref. [40]), including those with nontrivial topological properties [41], are found to possess \mathcal{PT} symmetry as well as other combined symmetries of \mathcal{T} and translation, rotation or mirror reflection operations. While candidate electronic materials are abundant, the simultaneous measurements of both $\sigma_{\mu\nu}^{\text{sc}}(\omega)$ and $\sigma_{\nu\mu}^{\text{cs}}(\omega)$ in these systems remain experimentally challenging. For this reason, quantum gases—with their significantly greater flexibility—provide an ideal platform to demonstrate these generalized Onsager relations as a proof of principle.

To showcase the versatility of these systems, we now use a single model of 2D spin-orbit-coupled atomic gases to illustrate all three categories of \mathcal{O} operations and the resulting generalized Onsager relations. Realized experimentally with both fermionic species ^{87}Sr [42] and bosonic species ^{87}Rb [43], the Hamiltonian of this model is

$$\hat{H} = \sum_{\sigma\sigma'} \int d\mathbf{r} \left(\hat{\psi}_\sigma^\dagger \hat{h}_{\sigma\sigma'} \hat{\psi}_{\sigma'} + \frac{g_{\sigma\sigma'}}{2} \hat{\psi}_\sigma^\dagger \hat{\psi}_{\sigma'}^\dagger \hat{\psi}_{\sigma'} \hat{\psi}_\sigma \right), \quad (12)$$

where $\hat{\psi}_\sigma^\dagger(\mathbf{r})$ ($\sigma = \uparrow, \downarrow$) creates a particle of spin σ , $g_{\sigma\sigma'}$ are the s -wave atomic interaction constants and \hat{h} is the single-particle Hamiltonian

$$\hat{h} = [\hat{p}^2/2m + V_{\text{latt}}(\hat{\mathbf{r}})] + V_{\text{R1}}(\hat{\mathbf{r}})\hat{s}_x + V_{\text{R2}}(\hat{\mathbf{r}})\hat{s}_y. \quad (13)$$

Here $V_{\text{latt}}(\hat{\mathbf{r}}) = V_0(\cos^2 k_L \hat{r}_x + \cos^2 k_L \hat{r}_y)$ is a 2D square optical lattice potential with potential depth V_0 and lattice separation π/k_L ; the spin-orbit coupling (SOC) is simulated using two Raman lattice potentials

TABLE I. Generalized Onsager relations in quantum gases

\mathcal{O}	\mathcal{P}	$C_{4z}^2 \mathcal{P}$	$C_{2\tau_2} \mathcal{P}$	$C_{2\tau_4} \mathcal{P}$
I_x	1	0	0	1
I_y	1	0	1	0
I_s	0	0	1	1
$(-1)^{I_{xx}}$	—	—	+	+
$(-1)^{I_{xy}}$	—	—	—	—
Fermi	✓	✓	✓	✓
Bose (phase I)	×	×	✓	✓
Bose (phase II)	×	✓	×	×

$V_{R1}(\mathbf{r}) = 2M_0 \sin(k_L \hat{r}_x) \cos(k_L \hat{r}_y)$ and $V_{R2}(\hat{\mathbf{r}}) = 2M_0 \sin(k_L \hat{r}_y) \cos(k_L \hat{r}_x)$, which couple the spatial degrees of freedom to the spin components $\hat{s}_x = \frac{1}{2}\sigma_x$ and $\hat{s}_y = \frac{1}{2}\sigma_y$.

A salient property of this model is that it possesses a high degree of symmetry [44–46], including the \mathcal{PT} symmetry and the modified dihedral symmetry \tilde{D}_4 . The latter is a double group whose 16 elements are spin-space rotations along various symmetry axes of the square lattice, i.e., $C_{4z}^n = e^{-i\frac{n\pi}{2}(\hat{s}_z + \hat{L}_z)}$ and $C_{2\tau_n} = e^{-i\pi\tau_n \cdot (\hat{s} + \hat{L})}$, where $\tau_n = \cos(n\pi/4)\hat{x} + \sin(n\pi/4)\hat{y}$ are in-plane unit vectors with $n = 1, 2, \dots, 8$. Here C_{4z} and $C_{2\tau_n}$, respectively, denote the four-fold rotation around the z -axis and the two-fold rotation around the in-plane vector τ_n . It can be verified that the single-particle Hamiltonian in Eq. (13) and the usual atomic interactions both commute with \mathcal{PT} and all elements of \tilde{D}_4 , and naturally with any combination of them. Thus the Hamiltonian has the \mathcal{OT} symmetry where $\mathcal{O} \in \mathcal{P}\tilde{D}_4$. Among the 16 elements of $\mathcal{P}\tilde{D}_4$, four operators have the properties in Eq. (4), which are \mathcal{P} , $C_{4z}^2 \mathcal{P} = e^{-i\pi\hat{s}_z}$, $C_{2\tau_2} \mathcal{P} = e^{-i\pi(\hat{s}_y + \hat{L}_x)}$ and $C_{2\tau_4} \mathcal{P} = e^{i\pi(\hat{s}_x + \hat{L}_y)}$. We see that the four \mathcal{O} operations indeed encompass all three categories previously mentioned. The transformations of \hat{r}_μ and \hat{s}_z under these operations are shown in the top part of Tab. I.

The ground states of this model, however, do not necessarily preserve all the symmetries of the Hamiltonian. Depending on particle statistics as well as atomic interactions, this Hamiltonian supports three types of ground states, each characterized by a different set of \mathcal{OT} symmetries. For spin- $\frac{1}{2}$ fermions with weak repulsive interactions, the ground state does not break any symmetry of the Hamiltonian and so the \mathcal{OT} symmetries with previously mentioned four \mathcal{O} operations are all present. As can be seen from Tab. I, the generalized Onsager relation for the longitudinal coefficients is symmetrical for \mathcal{P} and $C_{4z}^2 \mathcal{P}$ while antisymmetrical for $C_{2\tau_2} \mathcal{P}$ and $C_{2\tau_4} \mathcal{P}$. Thus we can infer immediately that $\sigma_{xx}^{\text{sc}}(\omega) = \sigma_{xx}^{\text{cs}}(\omega) = 0$ for the Fermi gas. The situation is different for the two-component Bose gas where the ground state necessarily breaks some symmetries of the Hamiltonian due to Bose-Einstein condensation. In fact, the interplay of SOC and atomic interaction lead to two phases distinguished by the magnetization, namely one with a perpendicular magnetization (phase I) and the other an in-plane magnetization (phase

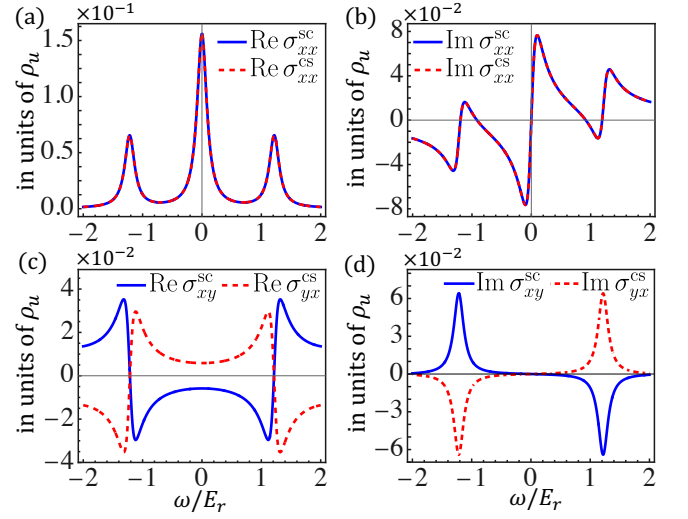


FIG. 1. Verification of the generalized Onsager relations for the Bose gas in perpendicularly magnetized phase (phase I). Here $V_0 = 4E_r$, $M_0 = 2.5E_r$, $\rho g_{\uparrow\uparrow} = 0.25E_r$ and $g_{\uparrow\downarrow}/g_{\uparrow\uparrow} = 0.9954$ (experimental ratio), where $\rho = N/A$ is the average atomic density and $E_r = k_L^2/2m$ is the recoil energy ($\hbar = 1$ throughout the paper). The conductivity tensors are in units of atom number per unit cell $\rho_u = 2\rho\pi^2/k_L^2$. A spectral broadening of $\eta = 0.1E_r$ is used in plotting.

II). These two phases can also be differentiated by which \mathcal{OT} symmetries they have retained [45, 46]. For the perpendicularly magnetized state (phase I), the condensate wave function $\Phi_I(\mathbf{r})$ is invariant with respect to both $C_{2\tau_2}\mathcal{PT}$ and $C_{2\tau_4}\mathcal{PT}$. In contrast, the condensate wave function $\Phi_{II}(\mathbf{r})$ for the in-plane magnetized state (phase II) only has the combined symmetry of $C_{4z}^2\mathcal{PT}$. These three ground states and their \mathcal{OT} symmetries are summarized in the lower part of Tab. I.

The Bose gas in phase I is particularly interesting because the generalized Onsager relation is symmetrical for the longitudinal dynamics but antisymmetrical for the transverse dynamics. We shall explicitly verify these relations by calculating the transport tensors without invoking the symmetry analysis. Unfortunately, the expressions in Eqs. (5)-(6) are inconvenient for a lattice system with periodic boundary conditions due to the fact that evaluating the matrix elements of the charge displacement operator \hat{R}_μ between the Bloch states involves some subtle difficulty [28]. Instead, the following equivalent formulas can be used [46]

$$\sigma_{\mu\nu}^{\text{sc}}(\omega) = \lim_{q \rightarrow 0} \partial_{q_\mu} \int_0^\infty dt \langle [\hat{\rho}^s(\mathbf{q}, t), \hat{j}_\nu^c(-\mathbf{q}, 0)] \rangle e^{i\omega t}; \quad (14)$$

$$\sigma_{\nu\mu}^{\text{cs}}(\omega) = \lim_{q \rightarrow 0} \partial_{q_\mu} \int_0^\infty dt \langle [\hat{j}_\nu^c(\mathbf{q}, t), \hat{\rho}^s(-\mathbf{q}, 0)] \rangle e^{i\omega t}, \quad (15)$$

where $\hat{\rho}^s(\mathbf{q}) = \sum_j \hat{s}_{j,z} e^{-i\mathbf{q} \cdot \hat{\mathbf{r}}_j}$ is the spin density and $\hat{j}_\nu^c(\mathbf{q}) = \frac{1}{2} \sum_j (\frac{d\hat{r}_{j,\nu}}{dt} e^{-i\mathbf{q} \cdot \hat{\mathbf{r}}_j} + e^{-i\mathbf{q} \cdot \hat{\mathbf{r}}_j} \frac{d\hat{r}_{j,\nu}}{dt})$ is the charge current density. For the Bose condensate, the spin density and charge current density operators can be expressed in terms of the quasi-particle operators under the Bogoliubov approxima-

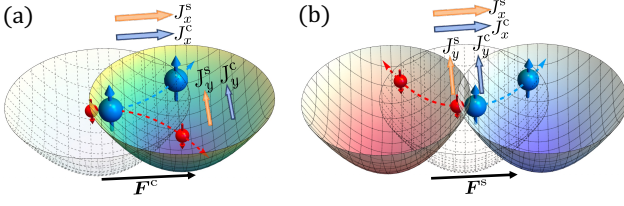


FIG. 2. Illustration of two experimental quench protocols that can be used to generate a force [protocol (a)] and a spin force [protocol (b)] along the x -direction in harmonically trapped quantum gases.

tion and their commutators can be evaluated once the excitation spectrum is determined [46, 47]. Shown in Fig. 1 are $\sigma_{\mu\nu}^{sc}(\omega)$ and $\sigma_{\nu\mu}^{cs}(\omega)$ calculated using Eqs. (14)-(15) for the SOC Bose gas in perpendicularly magnetized phase (phase I). These results show perfect agreement with the generalized Onsager relations given in Tab. I. We have also verified the generalized Onsager relations for the Fermi gas and the Bose gas in phase II, the details of which are relegated to the Supplemental Material [46].

Finally, we discuss how to test the generalized Onsager relations experimentally in cold atomic systems confined in an additional harmonic trapping potential $V_{tr}(\mathbf{r}) = m\omega_0^2\mathbf{r}^2/2$. Such trapped atomic systems are uniquely suited for the experimental study of these relations for two reasons. First, the forces conjugate to charge and spin displacements can be easily generated and controlled in experiments. For example, a spatially uniform force $\mathbf{F}^c(t) = \theta(t)m\omega_0^2\mathbf{d}$ can be produced by abruptly displacing the trapping potential a distance of \mathbf{d} at time $t = 0$, i.e., by quenching the trapping potential to $\tilde{V}_{tr}(\mathbf{r}) = V_{tr}(\mathbf{r} - \mathbf{d})$ [see Fig. 2(a)]. Similarly, a spin force $\mathbf{F}^s(t) = \theta(t)m\omega_0^2\mathbf{d}$ can be generated by replacing the trapping potential by two spin-selective potentials [48] separated by a distance of $2\mathbf{d}$, i.e., by quenching the trapping potential to $\tilde{V}_{tr}(\mathbf{r}) = V_{tr}(\mathbf{r} - \mathbf{d})|\uparrow\rangle\langle\uparrow| + V_{tr}(\mathbf{r} + \mathbf{d})|\downarrow\rangle\langle\downarrow|$ [see Fig. 2(b)]. Second, the coupled charge-spin dynamics can be conveniently probed by measuring the charge and spin displacements instead of the currents. According to the relation between the generalized coordinate and the currents, the spin displacement resulting from the quench protocol (a) in Fig. 2(a) is given by

$$R_\nu^{s(a)}(t) = \int_0^t dt' \int d\omega \sigma_{\nu\mu}^{sc}(\omega) F_\mu^c(\omega) e^{-i\omega t'} \quad (16)$$

and the charge displacement from the quench protocol (b) in Fig. 2(b) is

$$R_\mu^{c(b)}(t) = \int_0^t dt' \int d\omega \sigma_{\mu\nu}^{cs}(\omega) F_\nu^s(\omega) e^{-i\omega t'} \quad (17)$$

where $\mathbf{F}^{c(s)}(\omega) = \int dt \mathbf{F}^{c(s)}(t) e^{i\omega t}$. Assuming that both quenches are along the x -direction, we then have $\mathbf{F}^c(t) = \mathbf{F}^s(t) = \theta(t)m\omega_0^2 d\hat{x}$. Thus, the generalized Onsager relations for the Bose gas in phase I can be tested by examining whether the measured spin and charge displacements from

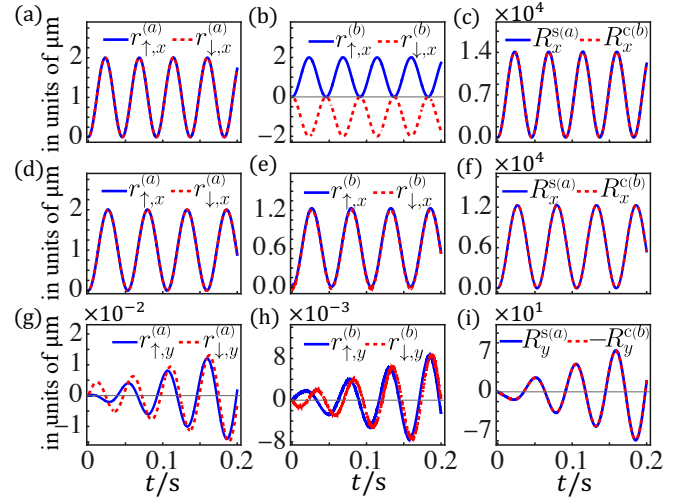


FIG. 3. The c.m. dynamics of the Bose gas in perpendicularly magnetized phase (phase I) during quench protocol (a) (the first column) and (b) (the second column). The first and the second row present the longitudinal dynamics of the independent two-component system ($M_0 = g_{\uparrow\downarrow} = 0$) and the SOC system respectively. The third row presents the transverse dynamics of the SOC system. Here the trap frequency is $\omega_0 = 2\pi \times 27\text{Hz}$, the total number of atoms is $N = 10^4$ and $g_{\uparrow\uparrow} = 1.946 \times 10^{-11}\text{Hzm}^2$. The rest of the parameters are the same as those in Fig. 1.

these two protocols satisfy the following relations

$$R_x^{s(a)}(t) = R_x^{c(b)}(t); \quad R_y^{s(a)}(t) = -R_y^{c(b)}(t). \quad (18)$$

This is to say that the longitudinal spin displacement resulting from quench protocol (a) must be exactly the same as the longitudinal charge displacement resulting quench protocol (b), while the corresponding transverse spin and charge displacements must be exactly opposite. To appreciate the highly non-trivial nature of the relations in Eq. (18), we first observe that the charge and spin displacements in experiments can be simply read out from the center of mass (c.m.) of the spin components $r_{\uparrow,\mu}$ and $r_{\downarrow,\mu}$, viz.,

$$R_\nu^{s(a)}(t) = N_\uparrow r_{\uparrow,\nu}^{(a)}(t) - N_\downarrow r_{\downarrow,\nu}^{(a)}(t); \quad (19)$$

$$R_\mu^{c(b)}(t) = N_\uparrow r_{\uparrow,\mu}^{(b)}(t) + N_\downarrow r_{\downarrow,\mu}^{(b)}(t), \quad (20)$$

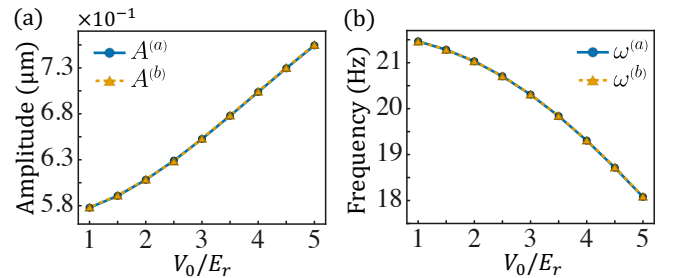


FIG. 4. Comparison of the amplitudes and frequencies between $R_x^{s(a)}(t) = A^{(a)} \sin \omega^{(a)} t$ and $R_x^{c(b)}(t) = A^{(b)} \sin \omega^{(b)} t$ for various lattice depths.

where N_\uparrow and N_\downarrow are the numbers of spin-up and spin-down atoms respectively. The first relation in Eq. (18) can be understood if there is no atomic interaction and no SOC at all, in which case the dynamics of the c.m. of the two spin components are completely independent. It is clear from the two protocols that $r_{\uparrow,x}^{(a)}(t) = r_{\uparrow,x}^{(b)}(t)$ and $r_{\downarrow,x}^{(a)}(t) = -r_{\downarrow,x}^{(b)}(t)$, which yields $R_x^{s(a)}(t) = R_x^{c(b)}(t)$ in light of Eqs. (19)-(20) [see Fig. 3(a)-(c)]. Now, the prediction of the generalized Onsager relations is that this must always be the case for any system parameter as long as the ground state of the system has the required symmetry. To verify this, we numerically simulate the c.m. dynamics of these two quench protocols using the time-dependent Gross-Pitaevskii equation [49]

$$i\partial_t \Phi_\sigma = \sum_{\sigma'} [(h_{\sigma\sigma'} + \tilde{V}_{\text{tr}} \delta_{\sigma\sigma'}) \Phi_{\sigma'} + g_{\sigma\sigma'} |\Phi_{\sigma'}|^2 \Phi_\sigma], \quad (21)$$

where $\Phi(\mathbf{r}, t) = (\Phi_\uparrow(\mathbf{r}, t), \Phi_\downarrow(\mathbf{r}, t))^T$ is the time-dependent condensate wave function. The c.m. dynamics of the spin components are calculated by $r_{\sigma,\mu}(t) = \frac{1}{N_\sigma} \int d\mathbf{r} r_{\mu} |\Phi_\sigma(\mathbf{r}, t)|^2$ and are shown in the first [protocol (a)] and second column [protocol (b)] of Fig. 3. In contrast to the case of independent two-component [Fig. 3(a)-(b)], we see that $r_{\uparrow,x}^{(a)}(t) \neq r_{\uparrow,x}^{(b)}(t)$ and $r_{\downarrow,x}^{(a)}(t) \neq -r_{\downarrow,x}^{(b)}(t)$ when atomic interactions and SOC are present [Fig. 3(d)-(e)]. In fact, the strong coupling of the two spin components is most clearly seen in Fig. 3(e), where the c.m. dynamics of the two components are almost synchronized even though the spin force is meant to drive them apart. Nevertheless, the first relation in Eq. (18) is perfectly satisfied as shown in Fig. 3(f). Furthermore, by comparing the amplitudes and frequencies of $R_x^{s(a)}(t)$ and $R_x^{c(b)}(t)$ for various lattice depths (see Fig. 4), we have demonstrated that the validity of the generalized Onsager relation is indeed independent of specific system parameters. The second relation in Eq. (18) describing the transverse charge-spin dynamics is similarly confirmed in Fig. 3(g)-(i), where we find that $R_y^{s(a)}(t)$ and $R_y^{c(b)}(t)$ are exactly opposite to each other. In this respect, the protocol (a) and (b) actually realize the spin Hall effect and its reciprocal process, the inverse spin Hall effect, respectively. Finally, we have confirmed that Eq. (18) holds even when thermal dissipation is present [46], suggesting that these relations can be experimentally tested at finite temperatures.

In conclusion, we have shown that the Onsager reciprocal relations of charge and spin transport can be generalized to systems breaking the time-reversal symmetry \mathcal{T} but preserving certain composite \mathcal{OT} symmetry. As a conceptual example, we have explicitly verified the generalized Onsager relations for a simple quantum gas SOC model and discussed intriguing experimental implication of these relations. For many solid state materials, our generalization reveals a hidden symmetry or antisymmetry between the charge-spin cross-coupling coefficients that may be useful in future studies of spintronics.

Acknowledgements This work is supported by Natural Science Foundation of China (Grant No. 12474264,

No. 12174455), Guangdong Provincial Quantum Science Strategic Initiative (Grant No. GDZX2404007), National Key R&D Program of China (Grant No. 2022YFA1404103), Natural Science Foundation of Guangdong Province (Grant No. 2021B1515020026), and Guangdong Basic and Applied Basic Research Foundation (Grant No. 2023B1515040023). S.Z. acknowledges support from HK GRF (Grant No. 17306024), CRF (Grants No. C6009-20G and No. C7012-21G), and a RGC Fellowship Award No. HKU RFS2223-7S03.

* These authors contributed equally to this work.

† yanzhib5@mail.sysu.edu.cn

‡ wuzhigang@quantumsc.cn

- [1] L. Onsager, Reciprocal Relations in Irreversible Processes. I., *Phys. Rev.* **37**, 405 (1931).
- [2] L. Onsager, Reciprocal Relations in Irreversible Processes. II., *Phys. Rev.* **38**, 2265 (1931).
- [3] H. B. G. Casimir, On Onsager's Principle of Microscopic Reversibility, *Rev. Mod. Phys.* **17**, 343 (1945).
- [4] D. G. Miller, Thermodynamics of Irreversible Processes. The Experimental Verification of the Onsager Reciprocal Relations., *Chemical Reviews* **60**, 15 (1960).
- [5] F. Sharipov, Onsager-Casimir reciprocity relations for open gaseous systems at arbitrary rarefaction: II. Application of the theory for single gas, *Physica A: Statistical Mechanics and its Applications* **203**, 457 (1994).
- [6] D. Andrieux and P. Gaspard, Fluctuation theorem and Onsager reciprocity relations, *The Journal of Chemical Physics* **121**, 6167 (2004).
- [7] E. Brunet and A. Ajdari, Generalized Onsager relations for electrokinetic effects in anisotropic and heterogeneous geometries, *Phys. Rev. E* **69**, 016306 (2004).
- [8] P. Jacquod, R. S. Whitney, J. Meair, and M. Büttiker, Onsager relations in coupled electric, thermoelectric, and spin transport: The tenfold way, *Phys. Rev. B* **86**, 155118 (2012).
- [9] C. Gorini, R. Raimondi, and P. Schwab, Onsager Relations in a Two-Dimensional Electron Gas with Spin-Orbit Coupling, *Phys. Rev. Lett.* **109**, 246604 (2012).
- [10] B. Tóth and B. Valkó, Onsager Relations and Eulerian Hydrodynamic Limit for Systems with Several Conservation Laws, *Journal of Statistical Physics* **112**, 497 (2003).
- [11] K.-T. Chen and P. A. Lee, Violation of the Onsager relation for quantum oscillations in superconductors, *Phys. Rev. B* **79**, 180510 (2009).
- [12] J. Bhattacharya, S. Bhattacharyya, S. Minwalla, and A. Yarom, A theory of first order dissipative superfluid dynamics, *Journal of High Energy Physics* **2014**, 147 (2014).
- [13] X. Wang, J. Dobnikar, and D. Frenkel, Numerical Test of the Onsager Relations in a Driven System, *Phys. Rev. Lett.* **129**, 238002 (2022).
- [14] X. Guo, X. Li, Z. Zhu, and K. Behnia, Onsager reciprocal relation between anomalous transverse coefficients of an anisotropic antiferromagnet, *Phys. Rev. Lett.* **131**, 246302 (2023).
- [15] M. Tsang, Quantum Onsager relations, *Quantum Science and Technology* **10**, 015015 (2024).
- [16] J. Shi, P. Zhang, D. Xiao, and Q. Niu, Proper definition of spin current in spin-orbit coupled systems, *Phys. Rev. Lett.* **96**,

- 076604 (2006).
- [17] P. Zhang, Z. Wang, J. Shi, D. Xiao, and Q. Niu, Theory of conserved spin current and its application to a two-dimensional hole gas, *Phys. Rev. B* **77**, 075304 (2008).
 - [18] C. Xiao, J. Zhu, B. Xiong, and Q. Niu, Conserved spin current for the Mott relation, *Phys. Rev. B* **98**, 081401 (2018).
 - [19] D. Monaco and L. Ulčakar, Spin Hall conductivity in insulators with nonconserved spin, *Phys. Rev. B* **102**, 125138 (2020).
 - [20] C. Xiao and Q. Niu, Conserved current of nonconserved quantities, *Phys. Rev. B* **104**, L241411 (2021).
 - [21] T. Tamaya, T. Kato, and T. Misawa, [What is a proper definition of spin current? – Lessons from the Kane-Mele Model](#) (2024), [arXiv:2403.06472 \[cond-mat.mes-hall\]](#).
 - [22] J. Sinova, D. Culcer, Q. Niu, N. A. Sinitsyn, T. Jungwirth, and A. H. MacDonald, Universal intrinsic spin Hall effect, *Phys. Rev. Lett.* **92**, 126603 (2004).
 - [23] J. Sinova, S. O. Valenzuela, J. Wunderlich, C. H. Back, and T. Jungwirth, Spin Hall effects, *Reviews of Modern Physics* **87**, 1213 (2015).
 - [24] To be specific, we focus on the components of the spin conductivity tensor describing the transport of spin aligned along z -direction in response to forces in the xy -plane.
 - [25] N. Sugimoto, S. Onoda, S. Murakami, and N. Nagaosa, Spin Hall effect of a conserved current: Conditions for a nonzero spin Hall current, *Phys. Rev. B* **73**, 113305 (2006).
 - [26] H. Liu, J. H. Cullen, and D. Culcer, Topological nature of the proper spin current and the spin-Hall torque, *Phys. Rev. B* **108**, 195434 (2023).
 - [27] J. H. Cullen and D. Culcer, Spin-Hall effect due to the bulk states of topological insulators: Extrinsic contribution to the proper spin current, *Phys. Rev. B* **108**, 245418 (2023).
 - [28] H. Ma, J. H. Cullen, S. Monir, R. Rahman, and D. Culcer, Spin-Hall effect in topological materials: evaluating the proper spin current in systems with arbitrary degeneracies, *npj Spintronics* **2**, 55 (2024).
 - [29] T. Jungwirth, X. Marti, P. Wadley, and J. Wunderlich, Antiferromagnetic spintronics, *Nature Nanotechnology* **11**, 231 (2016).
 - [30] L. Šmejkal, Y. Mokrousov, B. Yan, and A. H. MacDonald, Topological antiferromagnetic spintronics, *Nature Physics* **14**, 242 (2018).
 - [31] V. Baltz, A. Manchon, M. Tsoi, T. Moriyama, T. Ono, and Y. Tserkovnyak, Antiferromagnetic spintronics, *Rev. Mod. Phys.* **90**, 015005 (2018).
 - [32] A. Dal Din, O. J. Amin, P. Wadley, and K. W. Edmonds, Antiferromagnetic spintronics and beyond, *npj Spintronics* **2**, 25 (2024).
 - [33] B. H. Rimmler, B. Pal, and S. S. P. Parkin, Non-collinear antiferromagnetic spintronics, *Nature Reviews Materials* **10**, 109 (2025).
 - [34] M. Seemann, D. Ködderitzsch, S. Wimmer, and H. Ebert, Symmetry-imposed shape of linear response tensors, *Phys. Rev. B* **92**, 155138 (2015).
 - [35] R. Luo, G. Benenti, G. Casati, and J. Wang, Onsager reciprocal relations with broken time-reversal symmetry, *Phys. Rev. Res.* **2**, 022009 (2020).
 - [36] J. Zhou, Y. Gao, and Q. Niu, [Generalized Onsager's Relation in Magnon Hall Effect and Its Implication](#) (2025), [arXiv:2501.02250 \[cond-mat.mes-hall\]](#).
 - [37] Y. Pan, C. Le, B. He, S. J. Watzman, M. Yao, J. Gooth, J. P. Heremans, Y. Sun, and C. Felser, Giant anomalous Nernst signal in the antiferromagnet YbMnBi₂, *Nature Materials* **21**, 203 (2022).
 - [38] L.-D. Yuan, Z. Wang, J.-W. Luo, and A. Zunger, Prediction of low-Z collinear and noncollinear antiferromagnetic compounds having momentum-dependent spin splitting even without spin-orbit coupling, *Phys. Rev. Mater.* **5**, 014409 (2021).
 - [39] L. Šmejkal, J. Sinova, and T. Jungwirth, Beyond Conventional Ferromagnetism and Antiferromagnetism: A Phase with Non-relativistic Spin and Crystal Rotation Symmetry, *Phys. Rev. X* **12**, 031042 (2022).
 - [40] S. Hayami, M. Yatsushiro, and H. Kusunose, Nonlinear spin Hall effect in \mathcal{PT} -symmetric collinear magnets, *Phys. Rev. B* **106**, 024405 (2022).
 - [41] P. Tang, Q. Zhou, G. Xu, and S.-C. Zhang, Dirac fermions in an antiferromagnetic semimetal, *Nature Physics* **12**, 1100 (2016).
 - [42] M.-C. Liang, Y.-D. Wei, L. Zhang, X.-J. Wang, H. Zhang, W.-W. Wang, W. Qi, X.-J. Liu, and X. Zhang, Realization of Qi-Wu-Zhang model in spin-orbit-coupled ultracold fermions, *Phys. Rev. Res.* **5**, L012006 (2023).
 - [43] W. Sun, B.-Z. Wang, X.-T. Xu, C.-R. Yi, L. Zhang, Z. Wu, Y. Deng, X.-J. Liu, S. Chen, and J.-W. Pan, Highly controllable and robust 2D spin-orbit coupling for quantum gases, *Phys. Rev. Lett.* **121**, 150401 (2018).
 - [44] G.-H. Huang, G.-Q. Luo, Z. Wu, and Z.-F. Xu, Interaction-induced topological Bogoliubov excitations in a spin-orbit-coupled Bose-Einstein condensate, *Phys. Rev. A* **103**, 043328 (2021).
 - [45] C. Chen, G.-H. Huang, and Z. Wu, Intrinsic anomalous Hall effect across the magnetic phase transition of a spin-orbit-coupled Bose-Einstein condensate, *Phys. Rev. Res.* **5**, 023070 (2023).
 - [46] See Supplemental Material for more details on the derivation of the alternative Kubo formulas, symmetry properties of the Bose gas in phase I and II, the verification of the generalized Onsager relations for the Fermi gas and the Bose gas in phase II, and the simulation of dissipative quench dynamics, which includes Ref. [50, 51].
 - [47] H. Tang, G.-H. Huang, S. Zhang, Z. Yan, and Z. Wu, Unconventional spin Hall effect in \mathcal{PT} -symmetric spin-orbit-coupled quantum gases, *Phys. Rev. A* **111**, L051301 (2025).
 - [48] L. J. LeBlanc and J. H. Thywissen, Species-specific optical lattices, *Phys. Rev. A* **75**, 053612 (2007).
 - [49] Y. Kawaguchi and M. Ueda, Spinor Bose-Einstein condensates, *Phys. Rep.* **520**, 253 (2012).
 - [50] G. D. Mahan, *Many-particle physics*, 3rd ed. (Springer New York, NY, 2013).
 - [51] M. Tsubota, K. Kasamatsu, and M. Ueda, Vortex lattice formation in a rotating Bose-Einstein condensate, *Phys. Rev. A* **65**, 023603 (2002).

Supplemental Material for “Generalized Onsager reciprocal relations of charge and spin transport”

Guan-Hua Huang,^{1,2,*} Hui Tang,^{3,*} Shizhong Zhang,⁴ Zhongbo Yan,^{5,†} and Zhigang Wu^{2,‡}

¹*Hefei National Laboratory, Hefei 230088, China*

²*Quantum Science Center of Guangdong-Hong Kong-Macao
Greater Bay Area (Guangdong), Shenzhen 508045, China*

³*Shenzhen Institute for Quantum Science and Engineering,
Southern University of Science and Technology, Shenzhen 518055, China*

⁴*Department of Physics and HKU-UCAS Joint Institute
for Theoretical and Computational Physics at Hong Kong,
University of Hong Kong, Hong Kong, China*

⁵*Guangdong Provincial Key Laboratory of Magnetoelectric Physics and Devices,
School of Physics, Sun Yat-Sen University, Guangzhou 510275, China*

This Supplemental Material includes the following sections: (I) Derivation of alternative Kubo formulas; (II) Generalized Onsager relations in the Fermi gas; (III) Generalized Onsager relations in the Bose gas; and (IV) Simulation of the dissipative quench dynamics.

I. DERIVATION OF ALTERNATIVE KUBO FORMULAS

In this section, we derive alternative Kubo formulas of spin-charge cross-coupling transport tensors in a lattice system, i.e., Eqs. (14)-(15) of the main text, and show that they are equivalent to Eqs. (5)-(6) of the main text. We first consider the spin-charge response coefficients $\sigma_{\mu\nu}^{\text{sc}}(\omega)$. In the presence of an external potential $V^c(\mathbf{r}, t)$ that couples to the charge, the spin current density is given by linear response theory as

$$j_{\mu}^{\text{s}}(\mathbf{q}, \omega) = \chi_{j_{\mu}^{\text{s}}, \rho^c}(\mathbf{q}, \omega) V^c(\mathbf{q}, \omega), \quad (\text{S1})$$

* These authors contributed equally to this work.

† yanzhb5@mail.sysu.edu.cn

‡ wuzhigang@quantumsc.cn

where $V^c(\mathbf{q}, \omega)$ is the Fourier transform of $V^c(\mathbf{r}, t)$, $\chi_{A,B}(\mathbf{q}, \omega)$ is the Fourier transform of the retarded response function

$$\chi_{A,B}(\mathbf{q}, t - t') \equiv -i\theta(t - t')\langle [\hat{A}(\mathbf{q}, t), \hat{B}(-\mathbf{q}, t')] \rangle, \quad (\text{S2})$$

and $A(\mathbf{q}, \omega) \equiv \int dt \langle \hat{A}(\mathbf{q}, t) \rangle e^{i\omega t}$ as per standard notation. Here $\hat{j}_\mu^s(\mathbf{q}, t)$ and $\hat{\rho}^c(\mathbf{q}, t)$ are the Fourier transforms of spin current operator

$$\hat{j}_\mu^s(\mathbf{r}, t) = \frac{d}{dt} [\hat{\psi}^\dagger(\mathbf{r}, t) r_\mu s_z \hat{\psi}(\mathbf{r}, t)]$$

and density operator

$$\hat{\rho}^c(\mathbf{r}, t) = \hat{\psi}^\dagger(\mathbf{r}, t) \hat{\psi}(\mathbf{r}, t)$$

respectively, where $\hat{\psi}(\mathbf{r}, t) = [\hat{\psi}_\uparrow(\mathbf{r}, t), \hat{\psi}_\downarrow(\mathbf{r}, t)]^T$. Making use of

$$\hat{j}_\mu^s(\mathbf{q}, t) = \frac{d}{dt} \int d\mathbf{r} \hat{\psi}^\dagger(\mathbf{r}, t) r_\mu s_z \hat{\psi}(\mathbf{r}, t) e^{-i\mathbf{q}\cdot\mathbf{r}} = \frac{d}{dt} i \partial_{q_\mu} \hat{\rho}^s(\mathbf{q}, t) \quad (\text{S3})$$

where

$$\hat{\rho}^s(\mathbf{q}, t) = \int d\mathbf{r} \hat{\psi}^\dagger(\mathbf{r}, t) s_z \hat{\psi}(\mathbf{r}, t) e^{-i\mathbf{q}\cdot\mathbf{r}} \quad (\text{S4})$$

is the Fourier transform of the spin density, we can alternatively write

$$j_\mu^s(\mathbf{q}, \omega) = \omega \partial_{q_\mu} \rho^s(\mathbf{q}, \omega) = \omega \partial_{q_\mu} [\chi_{\rho^s, \rho^c}(\mathbf{q}, \omega) V^c(\mathbf{q}, \omega)] \quad (\text{S5})$$

where we used the linear response result

$$\rho^s(\mathbf{q}, \omega) = \chi_{\rho^s, \rho^c}(\mathbf{q}, \omega) V^c(\mathbf{q}, \omega). \quad (\text{S6})$$

We now have two equivalent expressions, (S1) and (S5), for the spin current density. We shall show that in the limit of $\mathbf{q} \rightarrow 0$ the first leads to Eq. (5) and the second to Eq. (14) of the main text. To do so, we first note that the external potential $V^c(\mathbf{r}, t)$ generates a force $\mathbf{F}^c(\mathbf{r}, t) = -\nabla V^c(\mathbf{r}, t)$ from which we find

$$\mathbf{F}^c(\mathbf{q}, \omega) = -i\mathbf{q} V^c(\mathbf{q}, \omega) \quad (\text{S7})$$

and

$$V^c(\mathbf{q}, \omega) = i \sum_\nu \frac{q_\nu}{q^2} F_\nu^c(\mathbf{q}, \omega). \quad (\text{S8})$$

Substituting (S8) into (S1), we obtain

$$j_\mu^s(\mathbf{q}, \omega) = \sum_\nu i \frac{q_\nu}{q^2} \chi_{j_\mu^s, \rho^c}(\mathbf{q}, \omega) F_\nu^c(\mathbf{q}, \omega). \quad (\text{S9})$$

From the definition of the transport tensor $j_\mu^s(\mathbf{q}, \omega) = \sum_\nu \sigma_{\mu\nu}^{sc}(\mathbf{q}, \omega) F_\nu^c(\mathbf{q}, \omega)$, we find

$$\sigma_{\mu\nu}^{sc}(\mathbf{q}, \omega) = i \frac{q_\nu}{q^2} \chi_{j_\mu^s, \rho^c}(\mathbf{q}, \omega). \quad (\text{S10})$$

Since $\hat{\rho}^c(\mathbf{q} = 0, 0)$ is the total particle number operator and commutes with the total current $\hat{j}_\mu^s(\mathbf{q} = 0, t)$, i.e., $[\hat{j}_\mu^s(0, t), \hat{\rho}^c(0, 0)] = 0$, we find that $\chi_{j_\mu^s, \rho^c}(0, \omega) = 0$. Thus we have

$$\begin{aligned} \sigma_{\mu\nu}^{sc}(\omega) &\equiv \lim_{\mathbf{q} \rightarrow 0} \sigma_{\mu\nu}^{sc}(\mathbf{q}, \omega) \\ &= \lim_{q_\nu \rightarrow 0} \lim_{q_\mu \rightarrow 0} i \frac{q_\nu}{q^2} [\chi_{j_\mu^s, \rho^c}(\mathbf{q}, \omega) - \chi_{j_\mu^s, \rho^c}(0, \omega)] \\ &= i \partial_{q_\nu} \chi_{j_\mu^s, \rho^c}(\mathbf{q}, \omega) \Big|_{\mathbf{q}=0} \\ &= i \int_0^\infty dt \langle [\hat{j}_\mu^s(\mathbf{q}, t), \partial_{q_\nu} \hat{\rho}^c(-\mathbf{q}, 0)] \rangle e^{i\omega t} \Big|_{\mathbf{q}=0} \\ &\quad + i \int_0^\infty dt \langle [\partial_{q_\nu} \hat{j}_\mu^s(\mathbf{q}, t), \hat{\rho}^c(-\mathbf{q}, 0)] \rangle e^{i\omega t} \Big|_{\mathbf{q}=0}. \end{aligned} \quad (\text{S11})$$

We note that the second term represents a response induced by a constant external potential which must vanish; the remaining term is precisely the right hand side of Eq. (5) in the main text, expressed in second quantization form.

Next we can write (S5) as

$$j_\mu^s(\mathbf{q}, \omega) = \omega [\partial_{q_\mu} \chi_{\rho^s, \rho^c}(\mathbf{q}, \omega)] V^c(\mathbf{q}, \omega) + \omega \chi_{\rho^s, \rho^c}(\mathbf{q}, \omega) \partial_{q_\mu} V^c(\mathbf{q}, \omega). \quad (\text{S12})$$

It can be shown that $\chi_{\rho^s, \rho^c}(0, \omega) = 0$ due to the fact that $[\hat{\rho}^s(0, t), \hat{\rho}^c(0, 0)] = 0$. Thus in the limit that $\mathbf{q} \rightarrow 0$ we only need to consider the first term of (S12). We shall show that

$$\chi_{\rho^s, \rho^c}(\mathbf{q}, \omega) = \frac{1}{\omega} \sum_\nu q_\nu \chi_{\rho^s, j_\nu^c}(\mathbf{q}, \omega), \quad (\text{S13})$$

where $\hat{j}_\nu^c(\mathbf{q}, t) = \frac{d}{dt} \int d\mathbf{r} \hat{\psi}^\dagger(\mathbf{r}, t) r_\nu \hat{\psi}(\mathbf{r}, t) e^{-i\mathbf{q} \cdot \mathbf{r}}$ is the Fourier transform of charge current density operator. Taking the derivative of $\chi_{\rho^s, \rho^c}(\mathbf{q}, t - t')$ with respect to t' , we have

$$\frac{d}{dt'} \chi_{\rho^s, \rho^c}(\mathbf{q}, t - t') = i\delta(t - t') \langle [\hat{\rho}^s(\mathbf{q}, t), \hat{\rho}^c(-\mathbf{q}, t)] \rangle - i\theta(t - t') \langle [\hat{\rho}^s(\mathbf{q}, t), \partial_t \hat{\rho}^c(-\mathbf{q}, t')] \rangle. \quad (\text{S14})$$

The commutator in the first term vanishes. Using the continuity equation $\partial_t \hat{\rho}^c(\mathbf{q}, t) + i\mathbf{q} \cdot \hat{\mathbf{j}}^c(\mathbf{q}, t) = 0$, (S14) becomes

$$\begin{aligned} \frac{d}{dt'} \chi_{\rho^s, \rho^c}(\mathbf{q}, t - t') &= -i\theta(t - t') \langle [\hat{\rho}^s(\mathbf{q}, t), \sum_\nu i q_\nu \hat{j}_\nu^c(-\mathbf{q}, t')] \rangle \\ &= \sum_\nu i q_\nu \chi_{\rho^s, j_\nu^c}(\mathbf{q}, t - t') \\ &= \sum_\nu i q_\nu \int \chi_{\rho^s, j_\nu^c}(\mathbf{q}, \omega) e^{-i\omega(t-t')} d\omega. \end{aligned} \quad (\text{S15})$$

On the other hand, we also have

$$\frac{d}{dt'} \chi_{\rho^s, \rho^c}(\mathbf{q}, t - t') = \int i\omega \chi_{\rho^s, \rho^c}(\mathbf{q}, \omega) e^{-i\omega(t-t')} d\omega. \quad (\text{S16})$$

Comparing this with (S15), we arrive at (S13). Substituting (S13) into (S5), we find

$$j_\mu^s(\mathbf{q} \rightarrow 0, \omega) = \lim_{\mathbf{q} \rightarrow 0} \sum_\nu [\delta_{\mu\nu} \chi_{\rho^s, j_\nu^c}(\mathbf{q}, \omega) + q_\nu \partial_{q_\mu} \chi_{\rho^s, j_\nu^c}(\mathbf{q}, \omega)] V^c(\mathbf{q}, \omega). \quad (\text{S17})$$

We note that the first term vanishes because $\chi_{j_\nu^c, \rho^s}(0, \omega) = 0$. This latter expression vanishes because it represents the charge current response induced by a uniform Zeeman field. Lastly, using (S7), we find

$$j_\mu^s(\mathbf{q} \rightarrow 0, \omega) = \lim_{\mathbf{q} \rightarrow 0} \sum_\nu i \partial_{q_\mu} \chi_{\rho^s, j_\nu^c}(\mathbf{q}, \omega) F_\nu^c(\mathbf{q}, \omega) \quad (\text{S18})$$

which implies that

$$\sigma_{\mu\nu}^{\text{sc}}(\omega) = i \partial_{q_\mu} \chi_{\rho^s, j_\nu^c}(\mathbf{q}, \omega) \Big|_{\mathbf{q}=0}. \quad (\text{S19})$$

This is nothing but Eq. (14) of the main text.

Now, we consider the charge-spin response coefficients $\sigma_{\nu\mu}^{\text{cs}}(\omega)$. In the presence of a potential $V^s(\mathbf{r}, t)$ that couples to the spin, the perturbation to the Hamiltonian is $s_z V^s(\mathbf{r}, t)$. The charge current induced by such a spin-dependent potential is given by linear response theory as

$$j_\nu^c(\mathbf{q}, \omega) = \chi_{j_\nu^c, \rho^s}(\mathbf{q}, \omega) V^s(\mathbf{q}, \omega). \quad (\text{S20})$$

Just like the case of the charge force, we have $V^s(\mathbf{q}) = \sum_\mu i F_\mu^s(\mathbf{q}, \omega) q_\mu / q^2$. Using this in (S20) we find

$$j_\nu^c(\mathbf{q}, \omega) = \sum_\mu \chi_{j_\nu^c, \rho^s}(\mathbf{q}, \omega) \frac{i q_\mu}{q^2} F_\mu^s(\mathbf{q}, \omega). \quad (\text{S21})$$

This implies that

$$\sigma_{\nu\mu}^{\text{cs}}(\omega) = \lim_{q_\mu \rightarrow 0} \lim_{q_\nu \rightarrow 0} i \frac{q_\mu \chi_{j_\nu^c, \rho^s}(\mathbf{q}, \omega)}{q^2} = i \partial_{q_\mu} \chi_{j_\nu^c, \rho^s}(\mathbf{q}, \omega) \Big|_{\mathbf{q}=0}, \quad (\text{S22})$$

where $\chi_{j_\nu^c, \rho^s}(0, \omega) = 0$ is used. We see that this is simply Eq. (15) of the main text. Now we prove that (S22) is equivalent to Eq. (6) of main text. (S22) can be written as

$$\begin{aligned} \sigma_{\nu\mu}^{\text{cs}}(\omega) &= i \partial_{q_\mu} \left[\int_0^\infty dt \langle [\hat{j}_\nu^c(\mathbf{q}, t), \hat{\rho}^s(-\mathbf{q}, 0)] \rangle e^{i\omega t} \right]_{\mathbf{q}=0} \\ &= i \int_0^\infty dt \langle [\partial_{q_\mu} \hat{j}_\nu^c(\mathbf{q}, t), \hat{\rho}^s(-\mathbf{q}, 0)] \rangle e^{i\omega t} \Big|_{\mathbf{q}=0} \\ &\quad + i \int_0^\infty dt \langle [\hat{j}_\nu^c(\mathbf{q}, t), \partial_{q_\mu} \hat{\rho}^s(-\mathbf{q}, 0)] \rangle e^{i\omega t} \Big|_{\mathbf{q}=0}. \end{aligned} \quad (\text{S23})$$

The first term of (S23) again represents a current-related response induced by a uniform Zeeman field and so should vanish; the remaining term is exactly Eq. (6) of main text in second quantization.

Both (S19) and (S22) are convenient to use in a lattice system. The derivatives of the response functions can be carried out numerically by the method of central difference, or analytically by expressing the response functions in terms of the Green's functions.

II. GENERALIZED ONSAGER RELATIONS IN THE FERMI GAS

In this section, we provide more details on the band structure of the model [1], the evaluation of the charge-spin cross-coupling transport coefficients for a noninteracting Fermi gas, and the verification of the generalized Onsager relations in this system.

A. Band structure and symmetries

We first determine the Bloch bands of the noninteracting Hamiltonian using the plane-wave expansion. The Hamiltonian reads

$$h(\mathbf{r}) = \frac{\mathbf{p}^2}{2m} + V_{\text{latt}}(\mathbf{r}) + \frac{1}{2}V_{\text{R1}}(\mathbf{r})\sigma_x + \frac{1}{2}V_{\text{R2}}(\mathbf{r})\sigma_y, \quad (\text{S24})$$

where $\sigma_{x(y)}$ are Pauli matrix and $V_{\text{latt}}(\mathbf{r}) = V_0[\cos^2(k_L x) + \cos^2(k_L y)]$ is the lattice potential; $V_{\text{R1}}(\mathbf{r}) = 2M_0 \sin(k_L x) \cos(k_L y)$ and $V_{\text{R2}}(\mathbf{r}) = 2M_0 \sin(k_L y) \cos(k_L x)$ are the Raman potentials. For this purpose, $\mathbf{a}_1 = (1, 1)\pi/k_L$ and $\mathbf{a}_2 = (-1, 1)\pi/k_L$ are chosen as the primitive vectors, and the reciprocal primitive vectors \mathbf{b}_i are determined by $\mathbf{a}_i \cdot \mathbf{b}_i = 2\pi\delta_{ij}$. In the plane-wave basis $|\mathbf{k}, \mathbf{Q}, \sigma\rangle = |\mathbf{k}, \mathbf{Q}\rangle \otimes |\sigma\rangle$, where

$$\left\{ |\mathbf{k}, \mathbf{Q}\rangle \otimes |\sigma\rangle \left| \langle \mathbf{r} | \mathbf{k}, \mathbf{Q}\rangle = \frac{e^{i(\mathbf{k}+\mathbf{Q})\cdot\mathbf{r}}}{\sqrt{A}}; \mathbf{k} \in \text{BZ}; \mathbf{Q} = m\mathbf{b}_1 + n\mathbf{b}_2; m, n \in \mathbb{Z}; \sigma = \uparrow\downarrow \right\}, \quad (\text{S25})$$

A is the area of the system, the noninteracting Hamiltonian (S24) can be expressed as a \mathbf{k} -dependent matrix $h(\mathbf{k})$ whose elements are

$$h_{\mathbf{Q}\sigma, \mathbf{Q}'\sigma'}(\mathbf{k}) = \langle \mathbf{k}, \mathbf{Q}, \sigma | h(\mathbf{r}) | \mathbf{k}, \mathbf{Q}', \sigma' \rangle. \quad (\text{S26})$$

The Bloch bands $\epsilon_{n\mathbf{k}}$ and Bloch functions $\phi_{n\mathbf{k}} = [\phi_{n\mathbf{k}\uparrow}, \phi_{n\mathbf{k}\downarrow}]^T$ are then obtained by diagonalizing $h(\mathbf{k})$. All the Bloch bands are doubly degenerate and the lowest four bands are

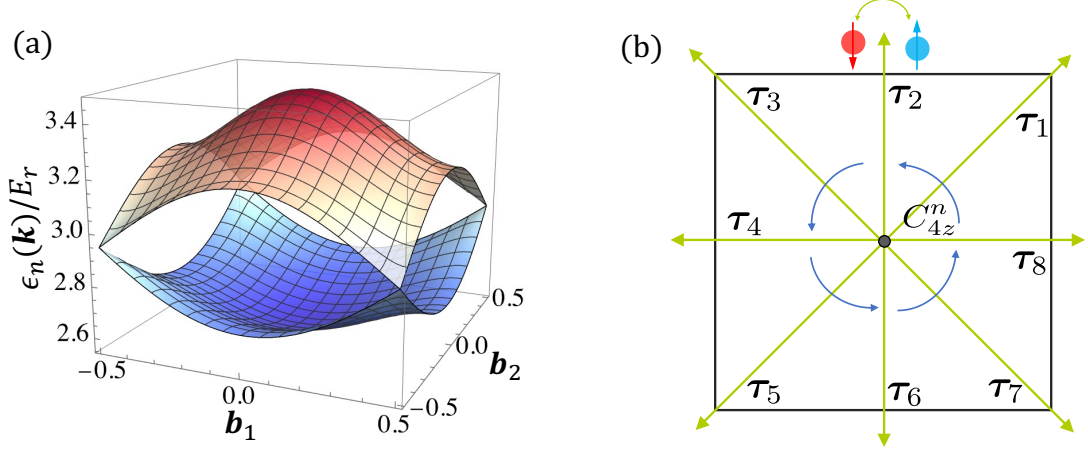


FIG. S1. (a) The lowest four Bloch bands in the first Brillouin zone (BZ), where the parameters are $V_0 = 4.0E_r$ and $M_0 = 2.0E_r$. (b) The illustration of the elements of the \tilde{D}_4 group.

shown Fig. S1(a). The double degeneracy is a direct consequence of the \mathcal{PT} symmetry of the Hamiltonian, where $\mathcal{P} = e^{-i\pi\hat{L}_z}$ is the two-dimensional spatial inversion and $\mathcal{T} = e^{-i\pi\hat{s}_y}\mathcal{K}$ (\mathcal{K} is the complex conjugation) is the time reversal operator for spin-1/2 systems. In addition to the \mathcal{PT} symmetry, the Hamiltonian (S24) also has the \tilde{D}_4 symmetry, which is a double group corresponding to the D_4 point group. The elements of \tilde{D}_4 are space-spin rotations along various symmetry axes of the square lattice, i.e., $C_{4z}^n = e^{-i\frac{n\pi}{2}(\hat{s}_z + \hat{L}_z)}$ and $C_{2\tau_n} = e^{-i\pi\tau_n \cdot (\hat{s} + \hat{L})}$, where $\tau_n = \cos(n\pi/4)\hat{x} + \sin(n\pi/4)\hat{y}$ are in-plane unit vectors with $n = 1, 2, \dots, 8$. [see Fig. S1(b)].

B. charge-spin cross-coupling transport coefficients

We now use (S19) to calculate $\sigma_{\mu\nu}^{\text{sc}}(\omega)$ for the noninteracting Fermi gas. The spin-current correlation function can be calculated by standard Matsubara method [2],

$$\chi_{\rho^s, j_\nu^c}(\mathbf{q}, \tau) = -\langle \mathcal{T} \hat{\rho}^s(\mathbf{q}, \tau) \hat{j}_\nu^c(-\mathbf{q}, 0) \rangle, \quad (\text{S27})$$

where $\tau \in [0, \beta)$ is the imaginary time, β is the inverse temperature and \mathcal{T} represents the time order operation. For practical calculations, we need to expand the field operator $\hat{\psi}(\mathbf{r}) = [\hat{\psi}_\uparrow(\mathbf{r}), \hat{\psi}_\downarrow(\mathbf{r})]^T$ in the plane wave basis (S25)

$$\hat{\psi}(\mathbf{r}) = \frac{1}{\sqrt{A}} \sum_{\mathbf{k} \in \text{BZ}, \mathbf{Q}} e^{i(\mathbf{k} + \mathbf{Q}) \cdot \mathbf{r}} \hat{\mathbf{c}}_{\mathbf{k}, \mathbf{Q}} \quad (\text{S28})$$

where $\hat{\mathbf{c}}_{\mathbf{k},\mathbf{Q}} = (\hat{c}_{\mathbf{k},\mathbf{Q},\uparrow}, \hat{c}_{\mathbf{k},\mathbf{Q},\downarrow})^T$. Defining $\hat{\boldsymbol{\psi}}_{\mathbf{k}} = (\hat{\mathbf{c}}_{\mathbf{k},\mathbf{Q}_1}^T, \hat{\mathbf{c}}_{\mathbf{k},\mathbf{Q}_2}^T, \dots)^T$, the noninteracting Hamiltonian (S24) can be written as

$$h = \sum_{\mathbf{k} \in \text{BZ}} \hat{\boldsymbol{\psi}}_{\mathbf{k}}^\dagger h(\mathbf{k}) \hat{\boldsymbol{\psi}}_{\mathbf{k}}, \quad (\text{S29})$$

and the spin density and charge current operators are

$$\hat{\rho}^s(\mathbf{q}) = \int d\mathbf{r} \hat{\boldsymbol{\psi}}^\dagger(\mathbf{r}) s_z \hat{\boldsymbol{\psi}}(\mathbf{r}) e^{-i\mathbf{q} \cdot \mathbf{r}} = \sum_{\mathbf{k} \in \text{BZ}} \hat{\boldsymbol{\psi}}_{\mathbf{k}}^\dagger S_z \hat{\boldsymbol{\psi}}_{\mathbf{k}+\mathbf{q}}, \quad (\text{S30})$$

$$\hat{j}_\nu^c(\mathbf{q}) = \frac{1}{2mi} \int d\mathbf{r} [\hat{\boldsymbol{\psi}}^\dagger(\mathbf{r}) \partial_\nu \hat{\boldsymbol{\psi}}(\mathbf{r}) - h.c.] e^{-i\mathbf{q} \cdot \mathbf{r}} = \sum_{\mathbf{k} \in \text{BZ}} \hat{\boldsymbol{\psi}}_{\mathbf{k}}^\dagger \partial_\nu h(\mathbf{k} + \mathbf{q}/2) \hat{\boldsymbol{\psi}}_{\mathbf{k}+\mathbf{q}}, \quad (\text{S31})$$

where $S_z = I_{N_{\mathbf{Q}}} \otimes s_z$, $N_{\mathbf{Q}}$ is the number of \mathbf{Q} index of the plane basis (S25) and I_N is an $N \times N$ identity matrix. Substituting (S30) and (S31) into (S27), we find

$$\chi_{\rho^s, j_\nu^c}(\mathbf{q}, \tau) = - \sum_{\mathbf{k}, \mathbf{k}' \in \text{BZ}} \langle \mathcal{T} \hat{\boldsymbol{\psi}}_{\mathbf{k}}^\dagger(\tau) S_z \hat{\boldsymbol{\psi}}_{\mathbf{k}+\mathbf{q}}(\tau) \hat{\boldsymbol{\psi}}_{\mathbf{k}'}^\dagger(0) \partial_\nu h(\mathbf{k}' - \mathbf{q}/2) \hat{\boldsymbol{\psi}}_{\mathbf{k}'-\mathbf{q}}(0) \rangle. \quad (\text{S32})$$

Considering the Fourier transform and using the Wick theorem, we have

$$\begin{aligned} \chi_{\rho^s, j_\nu^c}(\mathbf{q}, i\Omega_m) &= \int_0^\beta d\tau e^{i\Omega_m \tau} \chi_{\rho^s, j_\nu^c}(\mathbf{q}, \tau) \\ &= \sum_{\mathbf{k}, \mathbf{k}' \in \text{BZ}} \int_0^\beta d\tau e^{i\Omega_m \tau} \text{tr} S_z \langle \mathcal{T} \hat{\boldsymbol{\psi}}_{\mathbf{k}+\mathbf{q}}(\tau) \hat{\boldsymbol{\psi}}_{\mathbf{k}'}^\dagger(0) \rangle \partial_\nu h(\mathbf{k}' - \mathbf{q}/2) \langle \mathcal{T} \hat{\boldsymbol{\psi}}_{\mathbf{k}'-\mathbf{q}}(0) \hat{\boldsymbol{\psi}}_{\mathbf{k}}^\dagger(\tau) \rangle \\ &= \sum_{\mathbf{k} \in \text{BZ}} \int_0^\beta d\tau e^{i\Omega_m \tau} \text{tr} S_z G(\mathbf{k} + \mathbf{q}, \tau) \partial_\nu h(\mathbf{k} + \mathbf{q}/2) G(\mathbf{k}, -\tau) \\ &= \frac{1}{\beta} \sum_{\mathbf{k} \in \text{BZ}, n} \text{tr} S_z G(\mathbf{k} + \mathbf{q}, i\omega_n + i\Omega_m) \partial_\nu h(\mathbf{k} + \mathbf{q}/2) G(\mathbf{k}, i\omega_n), \end{aligned} \quad (\text{S33})$$

where $\Omega_m = 2m\pi/\beta$ and $\omega_n = (2n+1)\pi/\beta$ are the bosonic and fermionic Matsubara frequencies, respectively. Here

$$G(\mathbf{k}, \tau) = - \langle \mathcal{T} \hat{\boldsymbol{\psi}}_{\mathbf{k}}(\tau) \hat{\boldsymbol{\psi}}_{\mathbf{k}}^\dagger(0) \rangle = \frac{1}{\beta} \sum_n G(\mathbf{k}, i\omega_n) e^{-i\omega_n \tau} \quad (\text{S34})$$

is the imaginary time Green's function and

$$G(\mathbf{k}, i\omega_n) = \int_0^\beta d\tau G(\mathbf{k}, \tau) e^{i\omega_n \tau} = [i\omega_n - h(\mathbf{k})]^{-1} = \sum_n \frac{|\epsilon_{n,\mathbf{k}}\rangle \langle \epsilon_{n,\mathbf{k}}|}{i\omega_n - \epsilon_{n,\mathbf{k}}}, \quad (\text{S35})$$

where $|\epsilon_{n,\mathbf{k}}\rangle$ (the ket notation for the Bloch state $\phi_{n\mathbf{k}}$) is the eigenstate of $h(\mathbf{k})$ with energy $\epsilon_{n,\mathbf{k}}$. Substituting (S35) into (S33), we find

$$\chi_{\rho^s, j_\nu^c}(\mathbf{q}, i\Omega_m) = \frac{1}{\beta} \sum_{\mathbf{k} \in \text{BZ}, n, l, l'} \frac{\langle \epsilon_{l,\mathbf{k}} | S_z | \epsilon_{l',\mathbf{k}+\mathbf{q}} \rangle \langle \epsilon_{l',\mathbf{k}+\mathbf{q}} | \partial_\nu h(\mathbf{k} + \mathbf{q}/2) | \epsilon_{l,\mathbf{k}} \rangle}{(i\omega_n + i\Omega_m - \epsilon_{l',\mathbf{k}+\mathbf{q}})(i\omega_n - \epsilon_{l,\mathbf{k}})}. \quad (\text{S36})$$

Summing over the Matsubara frequency $i\omega_n$ and performing the analytic continuation $i\Omega_m \rightarrow \omega + i\eta$, (S36) becomes

$$\chi_{\rho^s, j_\nu^c}(\mathbf{q}, \omega) = \sum_{\mathbf{k} \in \text{BZ}, l, l'} \langle \epsilon_{l, \mathbf{k}} | S_z | \epsilon_{l', \mathbf{k}+\mathbf{q}} \rangle \langle \epsilon_{l', \mathbf{k}+\mathbf{q}} | \partial_\nu h(\mathbf{k} + \mathbf{q}/2) | \epsilon_{l, \mathbf{k}} \rangle \frac{f(\epsilon_{l, \mathbf{k}}) - f(\epsilon_{l', \mathbf{k}+\mathbf{q}})}{\omega + i\eta + \epsilon_{l, \mathbf{k}} - \epsilon_{l', \mathbf{k}+\mathbf{q}}}, \quad (\text{S37})$$

where η is an infinitesimal number but is taken to be a finite spectral broadening parameter later in the plots, $f(\epsilon_{l, \mathbf{k}}) = \frac{1}{e^{\beta(\epsilon_{l, \mathbf{k}} - \mu)} + 1}$ is the Fermi distribution function and μ is the chemical potential. Finally, the transport tensor (S19) can be calculated numerically by the central difference, i.e.,

$$\sigma_{\mu\nu}^{\text{sc}}(\omega) \approx \frac{\chi_{\rho^s, j_\nu^c}(\boldsymbol{\delta}_\mu, \omega) - \chi_{\rho^s, j_\nu^c}(-\boldsymbol{\delta}_\mu, \omega)}{2|\boldsymbol{\delta}_\mu|}, \quad (\text{S38})$$

where momentum $\boldsymbol{\delta}_\mu$ only contains μ -component and satisfies $|\boldsymbol{\delta}_\mu|/k_L \ll 1$. Similarly, we find

$$\chi_{j_\nu^c, \rho^s}(\mathbf{q}, \omega) = \sum_{\mathbf{k} \in \text{BZ}, l, l'} \langle \epsilon_{l, \mathbf{k}} | \partial_\nu h(\mathbf{k} + \mathbf{q}/2) | \epsilon_{l', \mathbf{k}+\mathbf{q}} \rangle \langle \epsilon_{l', \mathbf{k}+\mathbf{q}} | S_z | \epsilon_{l, \mathbf{k}} \rangle \frac{f(\epsilon_{l, \mathbf{k}}) - f(\epsilon_{l', \mathbf{k}+\mathbf{q}})}{\omega + i\eta + \epsilon_{l, \mathbf{k}} - \epsilon_{l', \mathbf{k}+\mathbf{q}}}, \quad (\text{S39})$$

from which we can calculate $\sigma_{\nu\mu}^{\text{cs}}(\omega)$ again by the central difference

$$\sigma_{\mu\nu}^{\text{cs}}(\omega) \approx \frac{\chi_{j_\nu^c, \rho^s}(\boldsymbol{\delta}_\mu, \omega) - \chi_{j_\nu^c, \rho^s}(-\boldsymbol{\delta}_\mu, \omega)}{2|\boldsymbol{\delta}_\mu|}. \quad (\text{S40})$$

C. Verification of the generalized Onsager relations

As we discussed in main text, the \mathcal{P} or $C_{4z}^2\mathcal{P}$ operations will lead to the generalized Onsager relations $\sigma_{xx}^{\text{sc}}(\omega) = -\sigma_{xx}^{\text{cs}}(\omega)$ and $\sigma_{xy}^{\text{sc}}(\omega) = -\sigma_{yx}^{\text{cs}}(\omega)$, while $C_{2\tau_2}\mathcal{P}$ or $C_{2\tau_4}\mathcal{P}$ operations will give rise to $\sigma_{xx}^{\text{sc}}(\omega) = \sigma_{xx}^{\text{cs}}(\omega)$ and $\sigma_{xy}^{\text{sc}}(\omega) = -\sigma_{yx}^{\text{cs}}(\omega)$. Combining these two sets of relations, we conclude that the transport coefficients for the Fermi gas must satisfy

$$\sigma_{xx}^{\text{sc}}(\omega) = \sigma_{xx}^{\text{cs}}(\omega) = 0, \quad \sigma_{xy}^{\text{sc}}(\omega) = -\sigma_{yx}^{\text{cs}}(\omega). \quad (\text{S41})$$

We now evaluate (S38) and (S40) for the Fermi gas in the insulator phase and show the results in Fig. S2. The vanishing longitudinal transport coefficients in Fig. S2(a)(b) and the antisymmetry of the transverse transport coefficients in Fig. S2(c)(d) are in complete agreement with the generalized Onsager relations (S41).

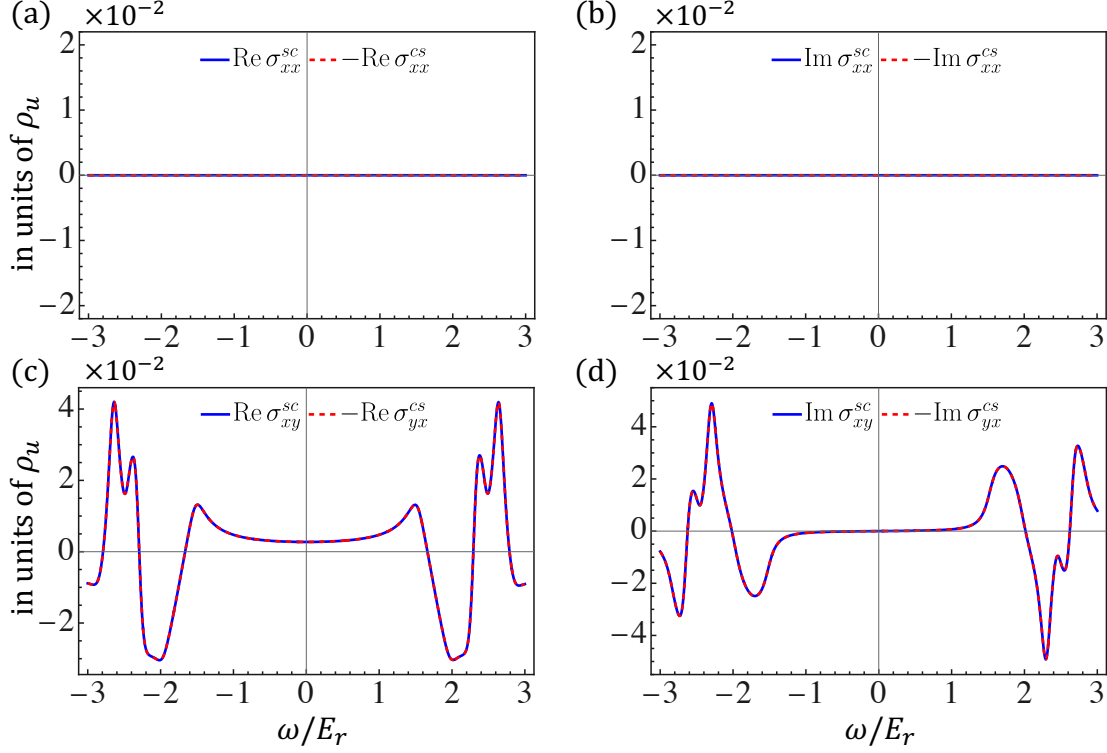


FIG. S2. Verification of the generalized Onsager relations for the Fermi gas in the insulator phase with $\rho_u = 4$. The rest of the parameters are $V_0 = 4.0E_r$, $M_0 = 2.0E_r$ and the spectral broadening $\eta = 0.1E_r$.

III. GENERALIZED ONSAGER RELATIONS IN THE BOSE GAS

In this section, we provide more details on the ground state symmetry properties of the Bose gas in phase I and II, the calculation of the transport tensors within the Bogoliubov framework, and the verification of the generalized Onsager relations in phase II. Although some of the information on the ground state symmetry and excitation spectrum can be found in Refs. [1, 3, 4], we sum them up here for the sake of completeness.

A. Meanfield ground states and their symmetries

The many-body Hamiltonian for the spin-orbited coupled Bose gas reads

$$\hat{H} = \sum_{\sigma\sigma'=\uparrow\downarrow} \int d\mathbf{r} \left[\hat{\psi}_{\sigma}^{\dagger}(\mathbf{r}) h_{\sigma\sigma'}(\mathbf{r}) \hat{\psi}_{\sigma'}(\mathbf{r}) + \frac{1}{2} g_{\sigma\sigma'} \hat{\psi}_{\sigma}^{\dagger}(\mathbf{r}) \hat{\psi}_{\sigma'}^{\dagger}(\mathbf{r}) \hat{\psi}_{\sigma'}(\mathbf{r}) \hat{\psi}_{\sigma}(\mathbf{r}) \right]. \quad (\text{S42})$$

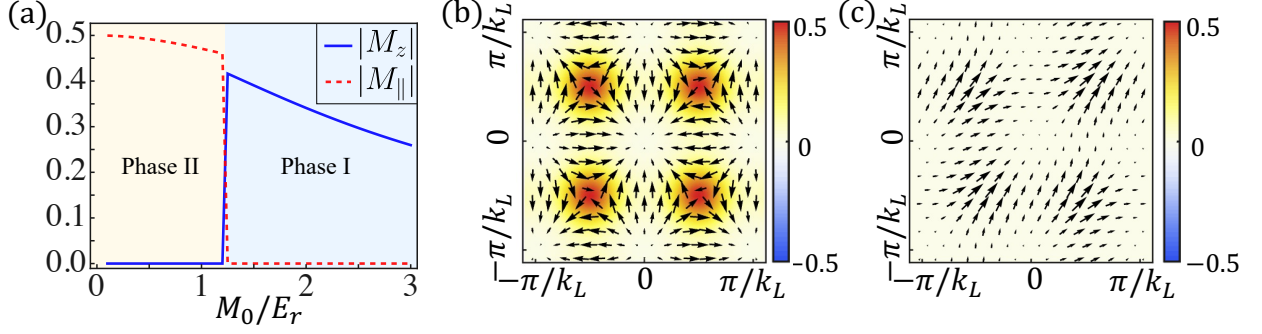


FIG. S3. (a) As the spin-orbit coupling strength M_0 decreases, the Bose gas undergoes a phase transition from the perpendicular magnetization phase (phase I) to the in-plane magnetization phase (phase II). (b) Magnetization density $\mathbf{m}(\mathbf{r})$ of Φ_+ mode in phase I with $M_0 = 2.0E_r$. The black arrows denote the x - and y -components of magnetization density and the background color represents the z -component. (c) Magnetization density $\mathbf{m}(\mathbf{r})$ of Φ_1 mode in phase II with $M_0 = 1.0E_r$. The rest of the parameters for these three plots are $V_0 = 4.0E_r$, $\rho g_{\uparrow\uparrow} = 0.25E_r$ and $\rho g_{\uparrow\downarrow} = 0.2E_r$.

At zero temperature, the condensate wave function $\langle\hat{\psi}(\mathbf{r})\rangle = [\langle\hat{\psi}_{\uparrow}(\mathbf{r})\rangle, \langle\hat{\psi}_{\downarrow}(\mathbf{r})\rangle]^T$ can be calculated by minimizing the Gross-Pitaevskii (GP) energy functional $\mathcal{E}(\{c_n\})$, which can be obtained by simply replacing $\hat{\psi}_{\sigma}$ and $\hat{\psi}_{\sigma}^{\dagger}$ by $\langle\hat{\psi}_{\sigma}(\mathbf{r})\rangle$ and $\langle\hat{\psi}_{\sigma}(\mathbf{r})\rangle$ respectively. Explicitly, we expand $\langle\hat{\psi}(\mathbf{r})\rangle$ in terms of the Bloch functions at the Γ point

$$\langle\hat{\psi}(\mathbf{r})\rangle = \Phi(\mathbf{r}) = \sqrt{N} \sum_n c_n \phi_{n0}(\mathbf{r}), \quad (\text{S43})$$

where N is the atom number of condensate. The coefficients $\{c_n\}$ can be determined by minimizing $\mathcal{E}(\{c_n\})$ and the chemical potential μ_B is given by $\partial\mathcal{E}/\partial N$. Two superfluid phases can be found for Hamiltonian (S42), i.e., the perpendicular magnetization phase (phase I) with magnetization along the z -direction, and the in-plane magnetization phase (phase II) with magnetization lying in the xy -plane [3]. Here the magnetization \mathbf{M} and the magnetization density \mathbf{m} are defined as

$$\mathbf{M} = \langle\Phi|\mathbf{s}|\Phi\rangle/N = \frac{1}{N} \int d\mathbf{r} \Phi^{\dagger}(\mathbf{r}) \mathbf{s} \Phi(\mathbf{r}) = \int d\mathbf{r} \mathbf{m}(\mathbf{r}), \quad (\text{S44})$$

where $\mathbf{s} = (s_x, s_y, s_z)$. The Bose gas in phase I spontaneously selects one of the two degenerate condensate modes Φ_{\pm} , distinguished by the magnetization $\mathbf{M} = |M_z|(0, 0, \pm 1)$. In phase II, it selects one of the four degenerate modes Φ_l distinguished by magnetization

$\mathbf{M} = |M_{\parallel}|(\cos \frac{(2l-1)\pi}{4}, \sin \frac{(2l-1)\pi}{4}, 0)$ ($l = 1, \dots, 4$) where $M_{\parallel} = \sqrt{M_x^2 + M_y^2}$. We show $|M_z|$ and M_{\parallel} as a function of M_0 in Fig. S3(a). In addition, we also show the magnetization densities of the condensate modes in phase I and II in Fig. S3(b) and (c).

Now we perform symmetry analysis on the condensate modes in phase I and II and determine what \mathcal{OT} symmetries they preserve. Since the Hamiltonian (S42) has \mathcal{PT} symmetry, there are at least two degenerate condensate wave functions $\Phi'(\mathbf{r})$ and $\Phi''(\mathbf{r}) = \mathcal{PT}\Phi'(\mathbf{r})$ for the Bose gas in either of the phases. The two states form a basis for a 2D irreducible representation $M^{(\tilde{g})}$ of \tilde{D}_4 group, where

$$\begin{pmatrix} M_{11}^{(\tilde{g})} & M_{12}^{(\tilde{g})} \\ M_{21}^{(\tilde{g})} & M_{22}^{(\tilde{g})} \end{pmatrix} = \begin{pmatrix} \langle \Phi' | \tilde{g} | \Phi' \rangle & \langle \Phi' | \tilde{g} | \Phi'' \rangle \\ \langle \Phi'' | \tilde{g} | \Phi' \rangle & \langle \Phi'' | \tilde{g} | \Phi'' \rangle \end{pmatrix}, \quad \forall \tilde{g} \in \tilde{D}_4. \quad (\text{S45})$$

According to Fig. S3(b), the condensate in phase I breaks $C_{2\tau_n}$ symmetries but preserves C_{4z}^n symmetries. So taking $\Phi' = \Phi_+$ we can infer that $C_{4z}^n \Phi' = e^{i\theta_{z,n}} \Phi'$ and

$$C_{2\tau_n} \Phi' = M_{11}^{(C_{2\tau_n})} \Phi' + M_{12}^{(C_{2\tau_n})} \Phi''. \quad (\text{S46})$$

Noting that in two dimensions $C_{4z}^2 C_{2\tau_n} C_{4z}^{2\dagger} = -C_{2\tau_n}$, we have

$$M_{11}^{(C_{2\tau_n})} = \langle \Phi' | C_{2\tau_n} | \Phi' \rangle = \langle \Phi' | C_{4z}^{2\dagger} C_{4z}^2 C_{2\tau_n} C_{4z}^{2\dagger} C_{4z}^2 | \Phi' \rangle = -\langle \Phi' | C_{2\tau_n} | \Phi' \rangle = 0. \quad (\text{S47})$$

Combining (S46) and (S47), we then find that $C_{2\tau_n} \Phi' = e^{i\theta_{\tau_n}} \Phi''$. On the other hand, $\Phi'' = \mathcal{PT}\Phi'$ and thus $C_{2\tau_n} \mathcal{PT}\Phi' = -e^{-i\theta_{\tau_n}} \Phi'$ which means that $C_{2\tau_n} \mathcal{PT}$ is a symmetry operation of the state Φ_+ in phase I. Although there is no restriction for τ_n here, there are only two distinctive \mathcal{O} operations that satisfy the conditions in Eq. (4) of the main text, i.e., $C_{2\tau_2} \mathcal{P} = e^{-i\pi(\hat{L}_x + \hat{s}_y)}$ and $C_{2\tau_4} \mathcal{P} = e^{i\pi(\hat{L}_y + \hat{s}_x)}$.

Next, we consider the Φ_1 mode in phase II (i.e., taking $\Phi' = \Phi_1$), which breaks C_{4z}^n symmetries but preserves $C_{2\tau_1}$ symmetry [see Fig. S3(b)]. Thus we can infer that $C_{2\tau_1} \Phi' = e^{i\theta_{\tau_1}} \Phi'$ and

$$C_{4z}^2 \Phi' = M_{11}^{(C_{4z}^2)} \Phi' + M_{12}^{(C_{4z}^2)} \Phi''. \quad (\text{S48})$$

Noting that in two dimensions $C_{2\tau_1} C_{4z}^2 C_{2\tau_1}^\dagger = -C_{4z}^2$, we have

$$M_{11}^{(C_{4z}^2)} = \langle \Phi' | C_{4z}^2 | \Phi' \rangle = \langle \Phi' | C_{2\tau_1}^\dagger C_{2\tau_1} C_{4z}^2 C_{2\tau_1}^\dagger C_{2\tau_1} | \Phi' \rangle = -\langle \Phi' | C_{4z}^2 | \Phi' \rangle = 0. \quad (\text{S49})$$

Combining (S48) and (S49), we find $C_{4z}^2 \Phi' = e^{i\theta_{z,2}} \Phi''$. Using $\Phi'' = \mathcal{PT}\Phi'$ again, we obtain that $C_{4z}^2 \mathcal{PT}\Phi' = -e^{-i\theta_{z,2}} \Phi'$ which indicates that $C_{4z}^2 \mathcal{PT}$ is a symmetry operation of the state Φ_1 . This is the only \mathcal{OT} symmetry we can identify for Φ_1 and thus the only \mathcal{O} operator for the condensate in the in-plane magnetized phase is $C_{4z}^2 \mathcal{P} = e^{-i\pi \hat{s}_z}$.

B. Bogoliubov excitations and the charge-spin transport tensors

Once the condensate wave function Φ obtained, we can substitute $\hat{\psi}_\sigma(\mathbf{r}) = \Phi_\sigma(\mathbf{r}) + \delta\hat{\psi}_\sigma(\mathbf{r})$ into the Hamiltonian (S42) to obtain Bogoliubov de Gennes (BdG) Hamiltonian

$$\hat{H}_B = \frac{1}{2} \int d\mathbf{r} \delta\hat{\psi}^\dagger(\mathbf{r}) \mathcal{H}(\mathbf{r}) \delta\hat{\psi}(\mathbf{r}), \quad (\text{S50})$$

where $\delta\hat{\psi}(\mathbf{r}) = [\delta\hat{\psi}_\uparrow(\mathbf{r}), \delta\hat{\psi}_\downarrow(\mathbf{r}), \delta\hat{\psi}_\uparrow^\dagger(\mathbf{r}), \delta\hat{\psi}_\downarrow^\dagger(\mathbf{r})]^T$ and

$$\mathcal{H}(\mathbf{r}) = \begin{pmatrix} h(\mathbf{r}) - \mu_B + \mathcal{M}(\mathbf{r}) & \mathcal{N}(\mathbf{r}) \\ \mathcal{N}^*(\mathbf{r}) & h^*(\mathbf{r}) - \mu_B + \mathcal{M}^*(\mathbf{r}) \end{pmatrix}, \quad (\text{S51})$$

$$\mathcal{M}(\mathbf{r}) = \begin{pmatrix} 2g_{\uparrow\uparrow}|\Phi_\uparrow|^2 + g_{\uparrow\downarrow}|\Phi_\downarrow|^2 & g_{\uparrow\downarrow}\Phi_\downarrow^*\Phi_\uparrow \\ g_{\uparrow\downarrow}\Phi_\uparrow^*\Phi_\downarrow & 2g_{\downarrow\downarrow}|\Phi_\downarrow|^2 + g_{\uparrow\downarrow}|\Phi_\uparrow|^2 \end{pmatrix}, \quad \mathcal{N}(\mathbf{r}) = \begin{pmatrix} g_{\uparrow\uparrow}\Phi_\uparrow^2 & g_{\uparrow\downarrow}\Phi_\downarrow\Phi_\uparrow \\ g_{\uparrow\downarrow}\Phi_\uparrow\Phi_\downarrow & g_{\downarrow\downarrow}\Phi_\downarrow^2 \end{pmatrix}. \quad (\text{S52})$$

We solve the BdG Hamiltonian (S50) in plane wave basis (S25). Specifically, we expand operator $\delta\hat{\psi}(\mathbf{r})$ as

$$\delta\hat{\psi}(\mathbf{r}) = \frac{1}{\sqrt{A}} \sum_{\mathbf{k} \in \text{BZ}, \mathbf{Q}} (\hat{c}_{\mathbf{k}, \mathbf{Q}}^T e^{i(\mathbf{k} + \mathbf{Q}) \cdot \mathbf{r}}, \hat{c}_{-\mathbf{k}, \mathbf{Q}}^\dagger e^{i(-\mathbf{k} + \mathbf{Q}) \cdot \mathbf{r}})^T. \quad (\text{S53})$$

Defining $\hat{\Psi}_{\mathbf{k}} = (\hat{\psi}_{\mathbf{k}}^T, \hat{\psi}_{-\mathbf{k}}^\dagger)^T$ and $\hat{\psi}_{\mathbf{k}} = (\hat{c}_{\mathbf{k}, \mathbf{Q}_1}^T, \hat{c}_{\mathbf{k}, \mathbf{Q}_2}^T, \dots)^T$, the BdG Hamiltonian can be written as $\hat{H}_B = \frac{1}{2} \sum_{\mathbf{k} \in \text{BZ}} \hat{\Psi}_{\mathbf{k}}^\dagger \mathcal{H}_{\mathbf{k}} \hat{\Psi}_{\mathbf{k}}$ where

$$\mathcal{H}_{\mathbf{k}} = \begin{pmatrix} h(\mathbf{k}) - \mu_B + \mathcal{M}(\mathbf{k}) & \mathcal{N}(\mathbf{k}) \\ \mathcal{N}^*(-\mathbf{k}) & h^*(-\mathbf{k}) - \mu_B + \mathcal{M}^*(-\mathbf{k}) \end{pmatrix}, \quad (\text{S54})$$

$$\mathcal{M}_{\mathbf{Q}_i, \mathbf{Q}_j}(\mathbf{k}) = \frac{1}{A} \int d\mathbf{r} \mathcal{M}(\mathbf{r}) e^{i(\mathbf{Q}_j - \mathbf{Q}_i) \cdot \mathbf{r}}, \quad \mathcal{N}_{\mathbf{Q}_i, \mathbf{Q}_j}(\mathbf{k}) = \frac{1}{A} \int d\mathbf{r} \mathcal{N}(\mathbf{r}) e^{-i(\mathbf{Q}_i + \mathbf{Q}_j) \cdot \mathbf{r}}. \quad (\text{S55})$$

Diagonalizing $\mathcal{H}_{\mathbf{k}}$ by an appropriate paraunitary matrix, we obtain the elementary excitations of the system.

To calculate the transport tensor (S19), we turn to the spin-current correlation function in the Bogoliubov framework. The spin operator (S30) and charge current operator (S31) in plane-wave basis and under the Bogoliubov approximation are

$$\hat{\rho}^s(\mathbf{q}) = \sum_{\mathbf{k} \in \text{BZ}} \hat{\psi}_{\mathbf{k}}^\dagger S_z \hat{\psi}_{\mathbf{k} + \mathbf{q}} = \frac{1}{2} \sum_{\mathbf{k} \in \text{BZ}} \hat{\Psi}_{\mathbf{k}}^\dagger \mathcal{S}_z \hat{\Psi}_{\mathbf{k} + \mathbf{q}} \approx \Psi_0^\dagger \mathcal{S}_z \hat{\Psi}_{\mathbf{q}}, \quad (\text{S56})$$

$$\hat{j}_\nu^c(\mathbf{q}) = \sum_{\mathbf{k} \in \text{BZ}} \hat{\psi}_{\mathbf{k}}^\dagger \partial_\nu h(\mathbf{k} + \frac{\mathbf{q}}{2}) \hat{\psi}_{\mathbf{k} + \mathbf{q}} = \frac{1}{2} \sum_{\mathbf{k} \in \text{BZ}} \hat{\Psi}_{\mathbf{k}}^\dagger \mathcal{J}_\nu^c(\mathbf{k} + \frac{\mathbf{q}}{2}) \hat{\Psi}_{\mathbf{k} + \mathbf{q}} \approx \hat{\Psi}_{-\mathbf{q}}^\dagger \mathcal{J}_\nu^c(-\frac{\mathbf{q}}{2}) \Psi_0. \quad (\text{S57})$$

where $\mathcal{S}_z = I_2 \otimes S_z$, $\mathcal{J}_\nu^c(\mathbf{q}) = \text{diag}(\partial_\nu h(\mathbf{q}), \partial_\nu h^*(\mathbf{k})|_{\mathbf{k}=-\mathbf{q}})$ and $\Psi_0 = [\langle \hat{\psi}_0^T \rangle, \langle \hat{\psi}_0^\dagger \rangle]^T$. Explicitly, $\langle \hat{\psi}_0^T \rangle = (\langle \hat{\mathbf{c}}_{0,\mathbf{Q}_1}^T \rangle, \langle \hat{\mathbf{c}}_{0,\mathbf{Q}_2}^T \rangle, \dots)$ with

$$\langle \hat{\mathbf{c}}_{0,\mathbf{Q}_i} \rangle = \frac{1}{\sqrt{A}} \int d\mathbf{r} \Phi(\mathbf{r}) e^{-i\mathbf{Q}_i \cdot \mathbf{r}}. \quad (\text{S58})$$

Using Eqs. (S56) and (S57), the spin-current correlation function can be written as

$$\chi_{\rho^s, j_\nu^c}(\mathbf{q}, \omega) = \Psi_0^\dagger \mathcal{S}_z \mathcal{G}(\mathbf{q}, \omega) \mathcal{J}_\nu^c(\mathbf{q}/2) \Psi_0, \quad (\text{S59})$$

where $\mathcal{G}(\mathbf{q}, \omega)$ is the retarded Green's function of the BdG Hamiltonian

$$\mathcal{G}(\mathbf{q}, \omega) = -i \int_0^\infty dt \langle [\Psi_{\mathbf{q}}(t), \Psi_{\mathbf{q}}^\dagger(0)] \rangle e^{(i\omega - \eta)t} = [(\omega + i\eta)\tau_z - \mathcal{H}_{\mathbf{q}}]^{-1}. \quad (\text{S60})$$

Here η again is a small positive quantity representing the spectral broadening and $\tau_z = \sigma_z \otimes I_{2N_{\mathbf{Q}}}$. Finally, the transport tensor is given by

$$\begin{aligned} \sigma_{\mu\nu}^{\text{sc}}(\omega) &= i \partial_{q_\mu} \chi_{\rho^s, j_\nu^c}(\mathbf{q}, \omega) \Big|_{\mathbf{q}=0} \\ &= \Psi_0^\dagger \mathcal{S}_z [\mathcal{G}(0, \omega) \tau_z \mathcal{J}_\mu^c(0) \mathcal{G}(0, \omega) \mathcal{J}_\nu^c(0) + \mathcal{G}(0, \omega) \partial_\mu \mathcal{J}_\nu^c(0)] \Psi_0 \end{aligned} \quad (\text{S61})$$

where $\partial_{\mathbf{q}} \mathcal{G} = -\mathcal{G}(\partial_{\mathbf{q}} \mathcal{G}^{-1}) \mathcal{G}$ and $\partial_{\mathbf{q}} \mathcal{G}^{-1}(\mathbf{q}) = -\partial_{\mathbf{q}} \mathcal{H}_{\mathbf{q}} = -\tau_z \mathcal{J}_\mu^c(\mathbf{q})$ have been used. Similarly, we find that the reciprocal tensor $\sigma_{\nu\mu}^{\text{cs}}(\omega)$ is given by

$$\begin{aligned} \sigma_{\nu\mu}^{\text{cs}}(\omega) &= i \partial_{q_\mu} \chi_{j_\nu^c, \rho^s}(\mathbf{q}, \omega) \Big|_{\mathbf{q}=0} \\ &= \Psi_0^\dagger [\partial_\mu \mathcal{J}_\nu^c(0) \mathcal{G}(0, \omega) + \mathcal{J}_\nu^c(0) \mathcal{G}(0, \omega) \tau_z \mathcal{J}_\mu^c(0) \mathcal{G}(0, \omega)] \mathcal{S}_z \Psi_0. \end{aligned} \quad (\text{S62})$$

C. Verification of the generalized Onsager relations in phase II

In the main text, we have used (S61) and (S62) to verify the generalized Onsager relations for the Bose gas in phase I. Here we also include the verification for the generalized Onsager relations for the Bose gas in phase II, which are

$$\sigma_{\mu\nu}^{\text{sc}}(\omega) = -\sigma_{\nu\mu}^{\text{cs}}(\omega). \quad (\text{S63})$$

The numerical results shown in Fig. S4 are in perfect agreement with the antisymmetry of the general Onsager relations (S63).

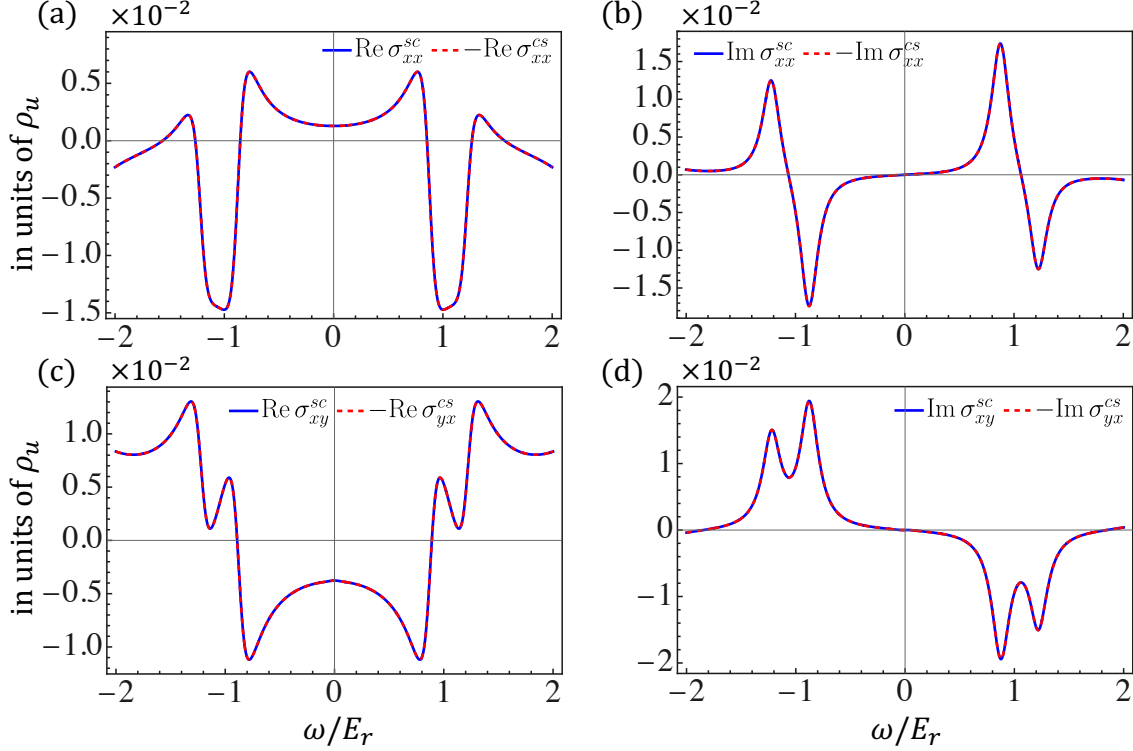


FIG. S4. Verification of the generalized Onsager relations for the Bose gas in the in-plane magnetized phase (phase II). Here the parameters are $V_0 = 4.0E_r$, $M_0 = 1.0E_r$, $\rho g_{\uparrow\uparrow} = 0.25E_r$, $\rho g_{\uparrow\downarrow} = 0.2E_r$ and the spectral broadening $\eta = 0.1E_r$.

IV. SIMULATION OF THE DISSIPATIVE QUENCH DYNAMICS

In the main text we have used the Gross-Pitaevskii (GP) equation to simulate experimental protocols for testing the generalized Onsager relations at zero temperature. Since any experiment is carried out at finite temperatures, it is useful to take into account the effects of dissipation in the GP simulation. In this section we repeat the simulations done in the main text but do so with the dissipative GP equation [5]

$$(i - \gamma)\partial_t \Phi_\sigma = \sum_{\sigma'} [(h_{\sigma\sigma'} + \tilde{V}_{\text{tr}}\delta_{\sigma\sigma'})\Phi_{\sigma'} + g_{\sigma\sigma'}|\Phi_{\sigma'}|^2\Phi_\sigma], \quad (\text{S64})$$

where γ is a phenomenological parameter that is often used to account for the effect of thermal dissipation.

As demonstrated in Fig. S5, the presence of dissipation leads to appreciable damping of the longitudinal oscillations. It also reduces the amplitude of the transverse dynamics as can be seen by a comparison of the third row of Fig. S5 with that of Fig. 3 in the main text.

Despite the significant effects of the dissipation, the generalized Onsager reciprocal relations are perfectly obeyed, as can be seen in (c), (f), and (i) of Fig. S5.

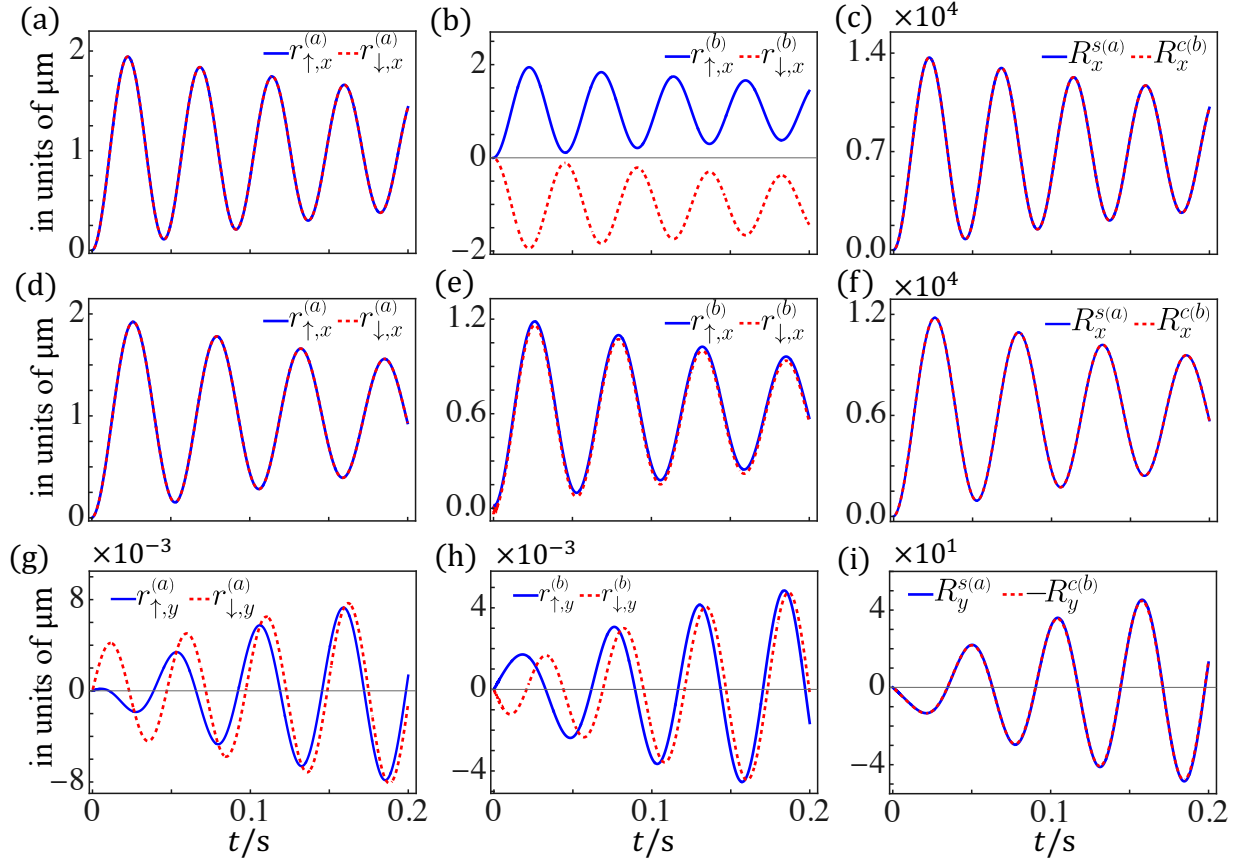


FIG. S5. The dissipated quench dynamics are simulated by the dissipative GP equation. The dissipation parameter is taken to be $\gamma = 0.005$; other parameters are the same as those in the main text.

-
- [1] G.-H. Huang, G.-Q. Luo, Z. Wu, and Z.-F. Xu, Interaction-induced topological Bogoliubov excitations in a spin-orbit-coupled Bose-Einstein condensate, [Phys. Rev. A **103**, 043328 \(2021\)](#).
 - [2] G. D. Mahan, [Many-particle physics](#), 3rd ed. (Springer New York, NY, 2013).
 - [3] C. Chen, G.-H. Huang, and Z. Wu, Intrinsic anomalous Hall effect across the magnetic phase transition of a spin-orbit-coupled Bose-Einstein condensate, [Phys. Rev. Res. **5**, 023070 \(2023\)](#).
 - [4] H. Tang, G.-H. Huang, S. Zhang, Z. Yan, and Z. Wu, Unconventional spin Hall effect in \mathcal{PT} -symmetric spin-orbit-coupled quantum gases, [Phys. Rev. A **111**, L051301 \(2025\)](#).

- [5] M. Tsubota, K. Kasamatsu, and M. Ueda, Vortex lattice formation in a rotating Bose-Einstein condensate, [Phys. Rev. A](#) **65**, 023603 (2002).